$Ru^{II}(bpy)_2L_2$ complexes. However, significantly better linear correlations are obtained when the monodentate and bidentate bonding types of sulfur-donor ligands are considered separately. This distinction is thought to arise from "chelation effect" contributions to the reorganizational energy terms and has not been as clearly demonstrated previously. Two dimeric complexes have been structurally characterized, and in both cases there is no discernible trans influence due to sulfur ligation.

Registry No. $Ru(bpy)_2WS_4$, 118831-60-0; $\{[Ru(bpy)_2]_2WS_4\}(PF_6)_2$, 118831-83-7; $Ru(bpy)_2(edt)_2$, 118831-61-1; $Ru(bpy)_2(SC_6H_5)_2$, 97279-25-9; $Ru(bpy)_2(SC_6H_4$-*p*-$CH_3)_2$, 118831-62-2; $Ru(bpy)_2(SC_6H_4$-*p*-$Cl)_2$, 118831-63-3; $Ru(bpy)_2(SC_4H_9)_2$, 118831-64-4; $Ru(bpy)_2(mnt)$, 118831-65-5; $Ru(bpy)_2(F_3CSO_3)_2$, 104474-95-5; $[(bpy)_2Ru(SC_6H_5)_2Ru(bpy)_2](F_3CSO_3)_2$, 118831-67-7; $Ru(bpy)_2S_5$, 118831-68-8; $Ru(bpy)_2(dmdmm)$, 118831-69-9; $[Ru(bpy)_2(CH_3CN)_2](Mo_2S_8)$, 118831-70-2; $Ru(bpy)_2Cl_2$, 15746-57-3; $(NH_4)_2WS_4$, 13862-78-7; $Ru(bpy)_2(SC_4H_9)_2^+$, 118831-71-3; $Ru(bpy)_2(SC_6H_4$-*p*-$CH_3)_2^+$, 118831-72-4; $Ru(bpy)_2(SC_6H_5)_2^+$, 97279-44-2; $Ru(bpy)_2(dmdmm)^+$, 118831-73-5; $Ru(bpy)_2(SC_6H_4$-*p*-$Cl)^+$, 118831-74-6; $Ru(bpy)_2(mnt)^+$, 118831-75-7; $Ru(bpy)_2(S_5)^+$, 118831-76-8; $Ru(bpy)_2(Mo_2S_4(S_2C_2H_4)_2)^+$, 118831-77-9; $Ru(bpy)_2(WS_4)^+$, 118831-81-5; $[Ru(bpy)_2(SC_6H_5)]_2^{4+}$, 118831-78-0; $\{[Ru(bpy)_2]_2WS_4\}^{4+}$, 118831-84-8; $Ru(bpy)_2(SC_5H_5)_2^+$, 118831-79-1; $Ru(bpy)_2(Mo_2S_4(S_2C_2H_4)_2)$, 118831-80-4; sulfur, 7704-34-9; dimethyl acetylenedicarboxylate, 762-42-5.

Supplementary Material Available: For both structures tables containing atom positional and thermal parameters, anisotropic thermal parameters, bond distances and angles, hydrogen atomic coordinates, and least-squares planes (58 pages); tables of structure factors (18 pages). Ordering information is given on any current masthead page.

Contribution from the Department of Chemistry,
State University of New York at Albany, Albany, New York 12222

Synthesis and Structural Investigation of Polyoxomolybdate Coordination Compounds Displaying a Tetranuclear Core. Crystal and Molecular Structures of $[n\text{-}Bu_4N]_2[Mo_4O_{10}(OMe)_4X_2]$ (X = -OMe, -Cl) and Their Relationship to the Catecholate Derivative $[n\text{-}Bu_4N]_2[Mo_4O_{10}(OMe)_2(OC_6H_4O)_2]$ and to the Diazenido Complexes of the *o*-Aminophenolate and the Naphthalene-2,3-diolate Derivatives $[n\text{-}Bu_4N]_2[Mo_4O_6(OMe)_2(HNC_6H_4O)_2(NNC_6H_5)_4]$ and $[n\text{-}Bu_4N]_2[Mo_4O_6(OMe)_2(C_{10}H_6O_2)_2(NNC_6H_5)_4]$. Comparison to the Structure of a Binuclear Complex with the $[Mo_2(OMe)_2(NNC_6H_5)_4]^{2+}$ Core, $[Mo_2(OMe)_2(H_2NC_6H_4O)_2(NNC_6H_5)_4]$

Hyunkyu Kang, Shuncheng Liu, Shahid N. Shaikh, Terrence Nicholson, and Jon Zubieta*

Received August 24, 1988

The tetranuclear methoxooxomolybdate $[MePPh_3]_2[Mo_4O_{10}(OCH_3)_6]$ ($[MePPh_3]_2[I]$) provides a synthetic precursor and a structural prototype for a class of tetranuclear polyoxomolybdate coordination complexes. Reaction of I with Me_3SiCl yields $[Mo_4O_{10}(OCH_3)_4Cl_2]^{2-}$ (II), which in turn may be reduced by thiols to yield a mixed-valence Mo(VI)/Mo(V) species, $[n\text{-}Bu_4N]_2[Mo_4O_8(OCH_3)_4Cl_4]$ ($[n\text{-}Bu_4N]_2[III]$). In the presence of chelating ligands, I reacts to give tetranuclear derivatives of the class $[n\text{-}Bu_4N]_2[Mo_4O_{10}(OCH_3)_2(LL)_2]$, where LL = catecholate ($[n\text{-}Bu_4N]_2[IVa]$), 3-*tert*-butylcatecholate ($[n\text{-}Bu_4N]_2[IVb]$), naphthalene-2,3-diolate ($[n\text{-}Bu_4N]_2[IVc]$), *o*-aminophenolate ($[n\text{-}Bu_4N]_2[IVd]$). Peripheral oxo groups of complexes IVa-d may be replaced by diazenido groups in condensation type reactions to give the tetranuclear complexes $[n\text{-}Bu_4N]_2[Mo_4O_6(OCH_3)_2(LL)_2(NNC_6H_5)_4]$ ($[n\text{-}Bu_4N]_2[Va\text{-}d]$). The related binuclear class of complexes $[Mo_2(OCH_3)_2(NNC_6H_5)_4(LL)_2]^n$ (VIa-d) has also been synthesized. Crystal data: I, triclinic, space group $P\bar{1}$, a = 10.185 (2) Å, b = 10.848 (2) Å, c = 11.686 (2) Å, α = 92.55 (2)°, β = 107.15 (2)°, γ = 96.79 (2)°, V = 1220.8 (6) Å^3, Z = 1, 2798 reflections (Mo Kα, λ = 0.710 73 Å in all cases), R = 0.0246; II, triclinic, space group $P\bar{1}$, a = 10.186 (4) Å, b = 11.722 (3) Å, c = 13.173 (4) Å, α = 109.35 (2)°, β = 107.43 (1)°, γ = 96.99 (1)°, V = 1372.6 (6) Å^3, Z = 1, 3020 reflections, R = 0.0407; III, monoclinic, space group $P2_1/n$, a = 10.653 (3) Å, b = 13.184 (4) Å, c = 12.703 (4) Å, β = 98.12 (1)°, V = 1766.1 (8) Å^3, Z = 2, 2424 reflections, R = 0.0469; IVa, monoclinic, space group $P2_1/a$, a = 18.494 (3) Å, b = 16.192 (4) Å, c = 20.411 (3) Å, β = 107.51 (1)°, V = 5822.6 (10) Å^3, Z = 4, 3832 reflections, R = 0.0566; Vc, rhombohedral, space group $R\bar{3}$ (hexagonal indices), a = 26.609 (4) Å, c = 31.844 (7) Å, V = 19 519.4 (9) Å^3, Z = 9, 2730 reflections, R = 0.0616; Vd, monoclinic, space group $P2_1/n$, a = 24.675 (2) Å, b = 19.937 (3) Å, c = 17.295 (4) Å, β = 112.62 (2)°, V = 7854.3 (11) Å, Z = 4, 4015 reflections, R = 0.0781; VId, triclinic, space group $P\bar{1}$, a = 9.500 (2) Å, b = 11.942 (3) Å, c = 12.026 (2) Å, α = 61.94 (1)°, β = 81.80 (2)°, γ = 86.11 (2)°, V = 1191.7 (10) Å^3, Z = 1, 2059 reflections, R = 0.0441.

Introduction

The interest in the chemistry of early-transition-metal polyanions derives in part from the structural analogies of these clusters to metal oxide surfaces[1,2] and from their industrial application as catalysts for selective air oxidation of organic molecules.[3] Furthermore, the chemistry of these polyoxometalate anions poses fundamental questions with respect to the elucidation of their reactivity and general coordination chemistry, of the mechanisms of interconversion of various structural types, and of their structural interrelationships. The recent expansion of the coordination chemistry of the polyoxometalates is a consequence of the availability of polyoxoanions soluble in organic solvents, displaying characteristic metal-ligand or organometallic reaction chemistry.[1] The reaction chemistry of polyoxometalate anion in nonaqueous solvents has been characterized by the replacement of peripheral oxo groups by organometallic units,[4-11] by a variety

* To whom correspondence should be addressed.

(1) Day, V. W.; Klemperer, W. G. *Science* **1985**, *228*, 533.
(2) Pope, M. T. *Heteropoly and Isopoly Oxometalates*; Springer-Verlag: New York, 1983.
(3) Matsuura, I.; Mizuno, S.; Hashiba, H. *Polyhedron* **1986**, *5*, 111.
(4) Che, T. M.; Day, V. W.; Francesconi, L. C.; Fredrick, M. F.; Klemperer, W. G.; Shum, W. *Inorg. Chem.* **1985**, *24*, 4055 and references therein.
(5) Besecker, C. J.; Day, V. W.; Klemperer, W. G.; Thompson, M. R. *Inorg. Chem.* **1985**, *24*, 44.

0020-1669/89/1328-0920$01.50/0

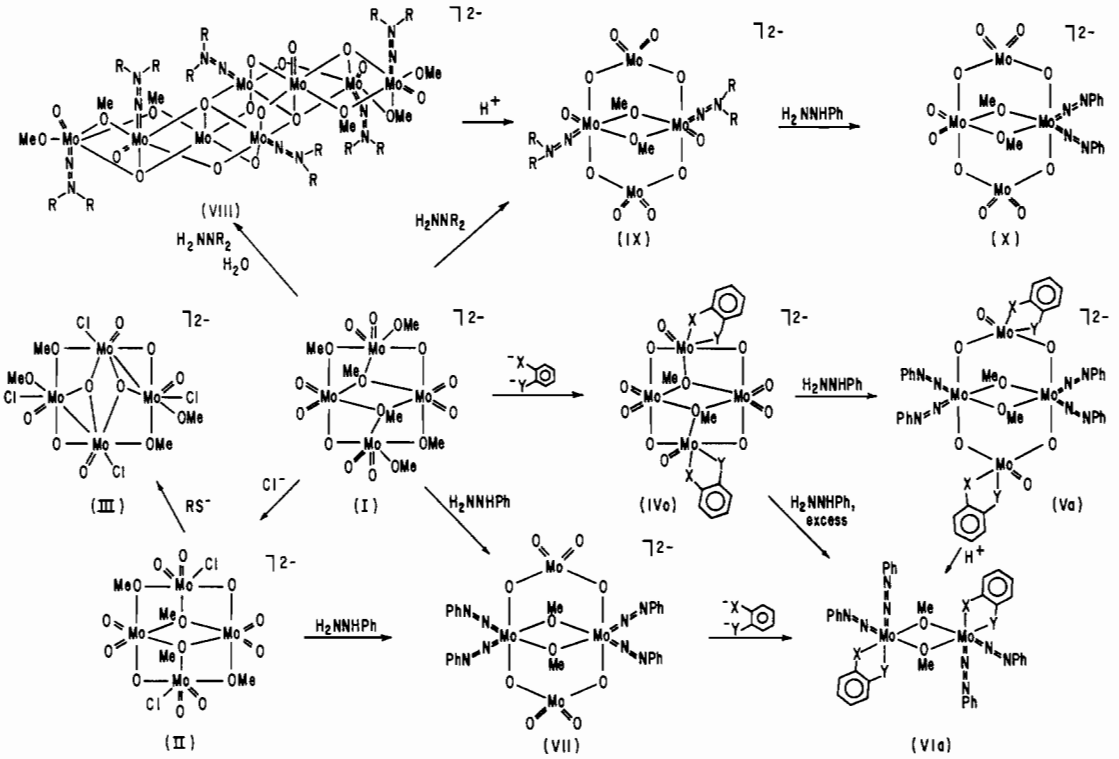

Figure 1. Schematic representation of the reaction chemistry of $[Mo_4O_{10}(OCH_3)_6]^{2-}$ and of derivative complexes that have been structurally characterized.

of simple organic ligands with oxygen,[12-18] nitrogen,[19-26] and sulfur donors,[27,28] and by inorganic ligands such as halide and sulfide donors.[29-31]

In the specific case of coordination complexes of polyoxomolybdate anions with oxygen-containing organic ligands, a number of alkoxo–isopolymolybdate species have been reported. The oxo–methoxo complex $[Mo_2O_5(OCH_3)_2]$[15] and the methoxo–isopolymolybdate $Na_4[Mo_8O_{24}(OCH_3)_4]\cdot 8CH_3OH$[14] provide chemical models and structural information relevant to surface coordination geometry in the selective oxidation of methanol to formaldehyde over molybdate catalysts, while alkoxo–isopolymolybdate complexes have been involved as models for selective hydrolysis of ethylene oxide to mono(ethylene glycol)[32,33] and for the general oxidation of primary and secondary alcohols.[34]

In the course of our investigations of the coordination chemistry of isopolymolybdate anions with organic ligands, we have isolated the tetranuclear methoxo–oxomolybdate cluster $[Mo_4O_{10}(OCH_3)_6]^{2-}$ (I). As summarized in Figure 1, $[Mo_4O_{10}(OCH_3)_6]^{2-}$ serves as the synthetic precursor in the preparation of a variety of structurally related organohydrazine,[20-24] alkoxide,[25] and halide derivatives.

In this paper, we present the details of the preparation of I and of its reaction with chloride to yield the isostructural tetranuclear species $[Mo_4O_{10}(OCH_3)_4Cl_2]^{2-}$ (II). Reaction of II with thiolate as a reducing agent yields the Mo(V)/Mo(VI) mixed-valence complex $[Mo_4O_8(OCH_3)_4Cl_4]^{2-}$ (III). The persistence of the tetranuclear core associated with I–III is further demonstrated by the isolation of complexes of the general type $[Mo_4O_{10}(OCH_3)_2(LL)_2]^{2-}$ (LL = catecholate, $(C_6H_4O_2)^{2-}$ (IVa); LL = 3-*tert*-butylcatecholate, $(Bu^tC_6H_3O_2)^{2-}$ (IVb); LL = naphthalene-2,3-diolate, $(C_{10}H_6O_2)^{2-}$ (IVc); LL = *o*-aminophenolate $(OC_6H_4NH)^{2-}$ (IVd)) from the reactions of I with the appropriate ligands. Peripheral oxo groups of complexes IVa–d exhibit the characteristic substitution reactions with phenylhydrazine in a condensation type reaction to give the species $[Mo_4O_6(OCH_3)_2(LL)_2(NNC_6H_5)_4]^{2-}$ (LL = $(C_6H_4O_2)^{2-}$ (Va), $(Bu^tC_6H_3O_2)^{2-}$ (Vb), $(C_{10}H_6O_2)^{2-}$ (Vc), $(OC_6H_4NH)^{2-}$ (Vd)). In the presence of excess phenylhydrazine, binuclear products of the general type $[Mo_2(OCH_3)_2(LL)_2(NNC_6H_5)_4]^n$ (VIa–d) are isolated. The

(6) Besecker, C. J.; Day, V. W.; Klemperer, W. G.; Thompson, M. R. *J. Am. Chem. Soc.* **1984**, *106*, 4125.
(7) Day, V. W.; Early, C. W.; Klemperer, W. G.; Maltbie, D. J. *J. Am. Chem. Soc.* **1985**, *107*, 8261.
(8) Besecker, C. J.; Klemperer, W. G.; Day, V. W. *J. Am. Chem. Soc.* **1982**, *104*, 6158.
(9) Day, V. W.; Klemperer, W. G.; Maltbie, D. J. *Organometallics* **1985**, *4*, 104.
(10) Klemperer, W. G.; Mainz, V. V.; Wang, R.-C.; Shum, W. *Inorg. Chem.* **1985**, *24*, 1968.
(11) Klemperer, W. G.; Liu, R.-S. *Inorg. Chem.* **1980**, *19*, 3863.
(12) Day, V. W.; Klemperer, W. G.; Schwartz, C. *J. Am. Chem. Soc.* **1987**, *109*, 6030.
(13) Adams, R. D.; Klemperer, W. G.; Liu, R.-S. *J. Am. Chem. Soc.* **1979**, *101*, 491. Day, V. W.; Thompson, M. R.; Day, C. S.; Klemperer, W. G.; Liu, R.-S. *J. Am. Chem. Soc.* **1980**, *102*, 5973.
(14) McCarron, E. M., III; Harlow, R. L. *J. Am. Chem. Soc.* **1983**, *105*, 6179.
(15) McCarron, E. M., III; Staley, H. H.; Sleight, W. *Inorg. Chem.* **1984**, *23*, 1043.
(16) McCarron, E. M., III; Sleight, A. W. *Polyhedron* **1986**, *5*, 129.
(17) Wilson, B. A.; Robinson, W. T.; Wilkins, C. J. *Acta Crystallogr.* **1983**, *C39*, 54.
(18) Liu, S.; Shaikh, S. N.; Zubieta, J. *Inorg. Chem.* **1987**, *26*, 4303.
(19) McCarron, E. M., III; Whitney, J. F.; Chase, D. B. *Inorg. Chem.* **1984**, *23*, 3276.
(20) Hsieh, T.-C.; Zubieta, J. *Inorg. Chem.* **1985**, *24*, 1287.
(21) Hsieh, T.-C.; Zubieta, J. *Polyhedron* **1986**, *5*, 309.
(22) Hsieh, T.-C.; Zubieta, J. *Polyhedron* **1986**, *5*, 1655.
(23) Shaikh, S. N.; Zubieta, J. *Inorg. Chem.* **1986**, *25*, 4613.
(24) Hsieh, T.-C.; Zubieta, J. *J. Chem. Soc., Chem. Commun.* **1985**, 1749.
(25) Hsieh, T.-C.; Shaikh, S. N.; Zubieta, J. *Inorg. Chem.* **1987**, *26*, 4079.
(26) Chilou, V.; Gouzerh, P.; Jeannin, Y.; Robert, F. *J. Chem. Soc., Chem. Commun.* **1987**, 1469.
(27) Hursthouse, M. B.; Short, R. L.; Piggott, B.; Tucker, A.; Wong, S. F. *Polyhedron* **1986**, *5*, 2122.
(28) Liu, S.; Sun, X.; Zubieta, J. *J. Am. Chem. Soc.* **1988**, *110*, 3324.
(29) Do, Y.; Simhon, E. D.; Holm, R. H. *Inorg. Chem.* **1985**, *24*, 2827.
(30) Klemperer, W. G.; Schwartz, C. *Inorg. Chem.* **1985**, *24*, 4459.
(31) Buchholz, N.; Mattes, R. *Angew. Chem., Int. Ed. Engl.* **1986**, *25*, 1104.
(32) Sheldon, R. A. *Recl. Trav. Chim. Pays-Bas* **1973**, *92*, 367.
(33) Briggs, J. R.; Harrison, A. M.; Robson, J. H. *Polyhedron* **1986**, *5*, 281.
(34) Kurusu, Y.; Masuyama, Y. *Polyhedron* **1986**, *5*, 289.
(35) Belicchi, M. F.; Fava, G. G.; Pelizzi, C. *J. Chem. Soc.* **1983**, 65.
(36) Beaver, J. A.; Drew, M. G. B. *J. Chem. Soc., Dalton Trans.* **1973**, 1376.

structures of I, II, III, IVa, Vc, Vd, and VId are discussed and compared to the structures of the previously reported binuclear and tetranuclear complexes with the $[Mo_2(OCH_3)_2(NNC_6H_5)_4]^{2+}$ core. The structural relationships of the tetranuclear core to the well-known β type octanuclear core and derivative structures are also presented.

Experimental Section

Materials and Methods. All preparations were carried out in freshly distilled dry solvents, and unless otherwise noted, no precautions to eliminate atmospheric oxygen were taken. Reagent grade solvents were used throughout. $(n\text{-}Bu_4N)_4[Mo_8O_{26}]$ was prepared by the literature method. All other reagents were obtained from standard commercial sources and used without further purification.

The following instruments were used in this work: IR, Perkin-Elmer 283B infrared spectrophotometer; UV–visible, Varian DMS 90 UV–visible spectrophotometer; electrochemistry, BAS100 electroanalytical system; X-ray crystallography, Nicolet R3m/V diffractometer and the MicroVAX II mounted solution package.

Elemental analyses were performed by Desert Analytics, Tucson, AZ.

Preparation of Compounds. $[Ph_3MeP]_2[Mo_4O_{10}(OCH_3)_6]$ ($[Ph_3MeP]_2$[I]). A solution of 1-methyl-1-phenylhydrazine (0.133 g, 0.872 mmol) in 30 mL of CH_2Cl_2–CH_3OH (1:1 v/v) was added to $[Ph_3MeP]_4[Mo_8O_{26}]$ (1.0 g, 0.43 mmol). After the solution was refluxed for 5 days, the color changed to reddish brown and 0.31 g of pale yellow precipitate was deposited. This pale yellow powder was dissolved in 30 mL of CH_2Cl_2–CH_3OH (1:1 v/v) at 50 °C and this mixture then filtered to produce a clear solution. Layering with 20 mL of HPLC grade heptane–anhydrous ether (1:1 v/v) and storing at −5 °C for 4 weeks gave very light yellow rectangular-shaped crystals. The crystals were washed with ether and vacuum-dried to yield 0.4 g of product (38% based on Mo). The crystals become opaque when exposed to an open atmosphere for a considerable time period. Anal. Calcd for $C_{44}H_{54}Mo_4O_{16}P_2$: C, 41.10; H, 4.21. Found: C, 41.03; H, 4.21. IR (KBr pellet, cm^{-1}): 3000 (m), 2940 (m), 2902 (m), 1437 (ms), 1111 (ms), 1060 (w), 1006 (ms), 926 (ms), 906 (vs), 885 (sh), 746 (s), 710 (br), 682 (s), 556 (ms), 510 (ms). ^{17}O NMR (CD_2Cl_2–CH_3OH (2:1), δ relative to $H_2{}^{17}O$): 946, 881, 572.

$[n\text{-}Bu_4N]_2[Mo_4O_{10}(OCH_3)_4Cl_2]$ ($[n\text{-}Bu_4N]_2$[II]). Method I. α-$[n\text{-}Bu_4N]_4[Mo_8O_{26}]$ (2.5 g, 1.16 mmol) was suspended in 100 mL of dry CH_3OH in a 250-mL three-necked flask fitted with a condenser. To this suspension was added PCl_5 (1.0 g, 4.8 mmol) very slowly through a Gooch flask. (*Caution*! Do not add PCl_5 abruptly, as the reaction is very exothermic.) After the addition of PCl_5, the reaction mixture was stirred at 25 °C for 20 h and then filtered to remove a white suspension. The transparent filtrate was evaporated to a light yellow viscous oil, which was dissolved in 30 mL of CH_2Cl_2, and this solution was layered with 2 mL of CH_3OH and 50 mL of ether. After 3 weeks at room temperature, a mixture of bright yellow crystals of $[n\text{-}Bu_4N]_2[Mo_6O_{19}]$ and transparent crystals of II was obtained. The crystals of complex II were separated from $[n\text{-}Bu_4N]_2[Mo_6O_{19}]$ in CCl_4 by the flotation method: $[n\text{-}Bu_4N]_2[Mo_6O_{19}]$ (ρ_{calc} = 1.78 g cm^{-3}) settled in a pool of CCl_4, while compound II (ρ_{calc} = 1.45 g cm^{-3}) floated on the liquid surface to effect separation. The crystals of II were washed with ether and vacuum-dried, yielding 1.04 g of air-stable product (35.4% based on Mo). The crystals decomposed to a white powder after prolonged exposure to the atmosphere. Anal. Calcd for $C_{36}H_{84}Cl_2Mo_4O_{14}N_2$: C, 35.33; H, 6.92; Cl, 5.79; N, 2.29. Found: C, 35.35; H, 7.10; Cl, 5.48; N, 2.26. IR (KBr pellet, cm^{-1}): 3000 (m), 2950 (ms), 2860 (m), 1480 (m), 1385 (w), 1025 (m), 1090 (m), 940 (s), 912 (vs), 895 (s), 735 (m, sh), 700 (s), 450 (m).

Method II. $(CH_3)_3SiCl$ (1.1 g, 10 mmol) was added dropwise to a solution of $[Ph_3MeP]_2[Mo_4O_{10}(OCH_3)_6]$ ($[Ph_3PMe]_2$[I]) (6.4 g, 5 mmol) in 100 mL of dry CH_3OH. After it was stirred at room temperature for 2 days, the colorless solution was filtered and an excess of $(n\text{-}Bu_4N)Cl$ (2.0 g) was added. When the mixture stood for 3 weeks, colorless translucent crystals of II were obtained in 1.5-g yield (24% based on Mo).

$[Et_3NH]_2[Mo_4O_8(OCH_3)_4Cl_4]$ ($[Et_3NH]_2$[III]). To a solution of $[n\text{-}Bu_4N]_2[Mo_4O_{10}(OCH_3)_4Cl_2]$ ($[n\text{-}Bu_4N]_2$[II]; 1.2 g, 1 mmol) in 25 mL of CH_3OH was added thiophenol (0.2 g, 2 mmol) and $(C_2H_5)_3N$ (0.2 g, 2 mmol). After it was stirred for 5 h, the deep red solution was concentrated to 10 mL and layered with diethyl ether. When the mixture stood at room temperature for 2 weeks, lustrous Chinese red crystals of III deposited in 0.4-g yield (40% based on Mo). Anal. Calcd for $C_{16}H_{44}N_2O_{12}Cl_4Mo_4$: C, 19.6; H, 4.48; N, 2.85. Found: C, 19.2; H, 4.35; N, 2.63. IR (KBr pellet, cm^{-1}): 2980 (m), 1640 (m), 1475 (m), 1390 (m), 1260 (m), 1035 (m), 960 (s), 940 (s), 795 (s), 725 (m), 675 (m), 490 (s).

$[n\text{-}Bu_4N]_2[Mo_4O_{10}(OCH_3)_2(OC_6H_4O)_2]$ ($[n\text{-}Bu_4N]_2$[IVa]). Catechol (0.44 g, 4 mmol) was added to a solution of α-$[Bu_4N]_4[Mo_8O_{26}]$ (2.2 g, 1.0 mmol) in 100 mL of warm CH_3OH. After it was stirred overnight, the solution was concentrated to 30 mL, whereupon 2.3 g of green powder was obtained. The crude product was dissolved in 15 mL of warm DMF, and this solution was then layered with MeOH. After the mixture stood at room temperature for 2 weeks, dark green crystals of IVa were obtained (1.8 g, 68% based on Mo). Anal. Calcd for $C_{46}H_{86}N_2Mo_4O_{16}$: C, 42.3; H, 6.63; N, 2.14. Found: C, 42.1; H, 6.75; N, 2.18. IR (KBr pellet, cm^{-1}): 2960 (s), 1470 (s), 1380 (m), 1330 (w), 1250 (s), 1001 (m), 935 (s), 910 (s), 730 (vs), 632 (s), 521 (m), 330 (m). UV/visible (CH_3CN; λ_{max}, nm (ϵ, cm^{-1} M^{-1})): 278 (2.8 × 10^3), 256 (2.2 × 10^3), 223 (3.4 × 10^3).

The analogous complexes $[n\text{-}Bu_4N]_2[Mo_4O_{10}(OCH_3)_2(Bu^tC_6H_3O_2)_2]$ ($[n\text{-}Bu_4N]_2$[IVb]), $[n\text{-}Bu_4N]_2[Mo_4O_{10}(OCH_3)_2(C_{10}H_6O_2)_2]$ ($[n\text{-}Bu_4N]_2$[IVc]), and $[n\text{-}Bu_4N]_2[Mo_4O_{10}(OCH_3)_2(OC_6H_4NH)_2]$ ($[n\text{-}Bu_4N]_2$[IVd]) were prepared by similar procedures, with the appropriate ligand precursors. For the complex IVb, the following analytical and spectroscopic parameters were obtained. Anal. Calcd for $C_{54}H_{102}N_2Mo_4O_{16}$: C, 45.70; H, 7.24; N, 1.97. Found: C, 45.72; H, 7.43; N, 1.89. IR (KBr pellet, cm^{-1}): 2950 (s), 1480 (s), 1280 (m), 1260 (s), 1000 (w), 940 (s), 910 (s), 750 (vs), 940 (s), 525 (m). UV/visible (CH_3CN; λ_{max}, nm (ϵ, cm^{-1} M^{-1})): 276 (1.66 × 10^3), 263 (1.6 × 10^3), 222 (2.91 × 10^3). For the complex IVc, the following analytical and spectroscopic parameters were obtained. Anal. Calcd for $C_{54}H_{90}N_2O_{16}Mo_4$: C, 46.1; H, 6.40; N, 1.99. Found: C, 46.0; H, 6.35; N, 1.87. IR (KBr pellet, cm^{-1}): 2955 (s), 1470 (s), 1300 (m), 1250 (s), 1000 (m), 935 (s), 905 (s), 740 (vs), 635 (s), 520 (m). UV/visible (CH_3CN; λ_{max}, nm (ϵ, cm^{-1} M^{-1})): 275 (2.01 × 10^3), 264 (2.1 × 10^3), 220 (270 × 10^3). For the complex IVd, the following analytical and spectroscopic parameters were obtained. Anal. Calcd for $C_{46}H_{88}N_4O_{14}Mo_4$: C, 42.3; H, 6.75; N, 4.30. found: C, 42.2; H, 6.70; N, 4.22. IR (KBr pellet, cm^{-1}): 3250 (w), 2960 (s), 1470 (s), 1350 (s), 1260 (s), 1000 (m), 940 (s), 910 (s), 740 (vs), 635 (s), 510 (m), 320 (m). UV/visible (CH_3CN; λ_{max}, nm (ϵ, cm^{-1} M^{-1})): 285 (1.9 × 10^3), 245 (2.0 × 10^3), 220 (3.5 × 10^3).

$[n\text{-}Bu_4N]_2[Mo_4O_6(OCH_3)_2(C_{10}H_6O_2)_2(NNC_6H_5)_4]$ ($[n\text{-}Bu_4N]_2$[IVc]). 2,3-Dihydroxynaphthalene (0.48 g, 3 mmol) was added to a solution of $[n\text{-}Bu_4N]_2[Mo_4O_8(OCH_3)_2(NNC_6H_5)_4]$ (1.58 g, 1 mmol) in CH_3OH–CH_2Cl_2 (50 mL, 1:1 v/v). After it was stirred at room temperature for 12 h, the deep purple solution was concentrated to 20 mL and layered with diethyl ether. When this mixture stood at room temperature for 2 weeks, dark red crystals of Vc were obtained in 0.53-g yield (30% based on Mo). Anal. Calcd for $C_{78}H_{110}N_{10}Mo_4O_{12}$: C, 53.12; H, 6.24; N, 7.95. Found: C, 52.78; H, 5.92; N, 7.58. IR (KBr pellet, cm^{-1}): 2960 (m), 1630 (w), 1570 (m), 1510 (s), 1465 (s), 1270 (s), 1020 (m), 940 (m), 890 (m), 765 (s), 625 (m), 565 (w). UV/visible (CH_3CN; λ_{max}, nm (ϵ, cm^{-1} M^{-1})): 518 (4.6 × 10^2), 456 (3.0 × 10^2), 248 (3.8 × 10^3).

The complexes $[n\text{-}Bu_4N]_2[Mo_4O_6(OCH_3)_2(C_6H_4O_2)_2(NNC_6H_5)_4]$ ($[n\text{-}Bu_4N]_2$[Va]) and $[n\text{-}Bu_4N]_2[Mo_4O_6(OCH_3)_2(Bu^tC_6H_3O_2)_2(NNC_6H_5)_4]$ ($[n\text{-}Bu_4N]_2$[Vb]) were prepared in a similar fashion.

$[n\text{-}Bu_4N]_2[Mo_4O_6(OCH_3)_2(OC_6H_4NH)_2(NNC_6H_5)_4]$ ($[n\text{-}Bu_4N]_2$[Vd]). Method I. To $[n\text{-}Bu_4N][MoO_2(C_6H_5(H)NNC(O)NNC_6H_5)(C_6H_5NNC(O)NNC_6H_5)]$ (1.5 g, 1.8 mmol) in 25 mL of CH_3OH was added an excess of phenylhydrazine (1.0 g, 9.2 mmol). When this solution was layered with diethylether and allowed to stand for 4 weeks, red block-shaped crystals were obtained in small yield (0.15 g, 20% based on Mo). Anal. Calcd for $C_{70}H_{108}N_{12}Mo_4O_{10}$: C, 50.6; H, 6.51; N, 10.12. Found: C, 49.9; H, 6.23; N, 9.85. IR (KBr pellet, cm^{-1}): 2950 (m), 1620 (w), 1565 (m), 1510 (s), 1475 (s), 1375 (w), 1260 (s), 920 (m), 760 (s), 725 (s), 630 (m), 560 (w).

Method II. $[n\text{-}Bu_4N]_2[Mo_4O_{10}(OCH_3)_2(OC_6H_4NH)_2]$ ($[n\text{-}Bu_4N]_2$[IVd]; 1.3 g, 1 mmol) in 50 mL of CH_3OH[3] was treated with phenylhydrazine (0.43 g, 4 mmol). After it was refluxed for 2 h, the deep purple solution was layered with diethyl ether and allowed to stand at room temperature for 2 weeks. Dark red crystals of Vd were obtained in 15% yield (0.25 g).

$[Mo_2(OCH_3)_2(OC_6H_4NH_2)_2(NNC_6H_4)_4]$·DMF (VId). 2-Aminophenol (0.44 g, 4 mmol) was added to a solution of $[n\text{-}Bu_4N]_2[Mo_4O_8(OCH_3)_2(NNC_6H_5)_4]$ (1.5 g, 1 mmol) in 50 mL of CH_3OH. After overnight stirring, filtration yielded 1.7 g of red powder, which was dissolved in 10 mL of DMF. Layering of this DMF solution with CH_3OH, followed by standing at room temperature for 2 weeks, yielded 1.3 g of VId (yield 63% based on Mo). Anal. Calcd for $C_{44}H_{50}N_{12}Mo_2O_4$: C, 51.1; H, 4.87; N, 16.3. Found: C, 51.5; H, 4.47; N, 15.9. IR (KBr pellet, cm^{-1}): 1668 (m), 1600 (m), 1505 (s), 1470 (s), 1280 (m), 1260 (w), 1130 (w), 750 (m). UV/visible (CH_3CN; λ_{max}, nm (ϵ, cm^{-1} M^{-1})): 519 (4.8 × 10^2), 456 (2.8 × 10^2), 301 (2.6 × 10^3), 292 (2.5 × 10^3).

The complexes $[n\text{-}Bu_4N]_2[Mo_2(OCH_3)_2(C_6H_4O_2)_2(NNC_6H_5)_4]$ ($[n\text{-}Bu_4N]_2$[VIa]), $[n\text{-}Bu_4N]_2[Mo_2(OCH_3)_2(Bu^tC_6H_3O_2)_2(NNC_6H_5)_4]$ ($[n\text{-}Bu_4N]_2$[VIb]), and $[n\text{-}Bu_4N]_2[Mo_2(OCH_3)_2(C_{10}H_6O_2)_2(NNC_6H_5)_4]$ ($[n\text{-}Bu_4N]_2$[VIc]) were obtained in reactions similar to that employed

Table I. Summary of Experimental Details for the X-ray Diffraction Studies of $[Ph_3PMe]_2[Mo_4O_{10}(OCH_3)_6]$ ($[Ph_3PMe]_2[I]$), $[Bu_4N]_2[Mo_4O_{10}(OCH_3)_4Cl_2]$ ($[Bu_4N]_2[II]$), $[Et_3NH]_2[Mo_4O_8(OCH_3)_4Cl_4]$ ($[Et_3NH]_2[III]$), $[Bu_4N]_2[Mo_4O_{10}(OCH_3)_2(OC_6H_4O)_2]$ ($[Bu_4N]_2[IVa]$), $[Bu_4N]_2[Mo_4O_6(OCH_3)_2(C_{10}H_6O_2)_2(NNC_6H_5)_4]$ ($[Bu_4N]_2[Vc]$), $[Bu_4N]_2[Mo_4O_6(OCH_3)_2(OC_6H_4NH)_2(NNC_6H_5)_4]$ ($[Bu_4N][Vd]$), and $[Mo_2(OCH_3)_2(OC_6H_4NH_2)_2(NNC_6H_5)_4]$ (VId)

	I	II	III	IVa	Vc	Vd	VId
T, K	296	296	296	296	296	296	296
a, Å	10.185 (2)	10.186 (4)	10.653 (3)	18.494 (3)	26.609 (4)	24.675 (2)	9.500 (2)
b, Å	10.848 (2)	11.722 (3)	13.184 (4)	16.192 (4)	26.609 (4)	19.937 (3)	11.942 (3)
c, Å	11.686 (2)	13.173 (4)	12.703 (4)	20.411 (3)	31.844 (7)	17.295 (4)	12.026 (2)
α, deg	92.55 (2)	109.35 (2)	90.00	90.00	90.00	90.00	61.94
β, deg	107.15 (2)	107.43 (1)	98.12 (1)	107.51 (1)	90.00	112.62 (2)	81.80 (2)
γ, deg	96.79 (2)	96.99 (1)	90.00	90.00	120.00	90.00	86.11 (2)
V, Å^3	1220.8 (6)	1372.6 (3)	1766.1 (8)	5822.6 (10)	19 519.4 (9)	7854.3 (11)	1191.7 (10)
space group	$P\bar{1}$	$P\bar{1}$	$P2_1/n$	$P2_1/a$	$R\bar{3}$	$P2_1/n$	$P\bar{1}$
Z	1	1	2	4	9	4	1
ρ_{calcd}, g cm^{-3}	1.73	1.45	1.84	1.49	1.35	1.40	1.44
cryst color and shape	light yellow block	light yellow block	orange needle	yellow block	black block	black needle	black block
cryst dimens, mm	0.32 × 0.25 × 0.35	0.25 × 0.33 × 0.18	0.25 × 0.45 × 0.18	0.22 × 0.20 × 0.26	0.32 × 0.31 × 0.37	0.21 × 0.37 × 0.18	0.25 × 0.27 × 0.25
no. of reflns collected	6864 ($+h,\pm k,\pm l$)	4660 ($+h,\pm k,\pm l$)	3645 ($+h,+k,\pm l$)	5645 ($+h,+k,\pm l$)	5865 ($\pm h,+k,+l$)	6727 ($+h,+k,\pm l$)	3380 ($+h,\pm k,\pm l$)
no. of rflns used in refinement, $F_o \geq 6.0\sigma(F_o)$	2798	3020	2424	3832	2730	4015	2059
no. of params refined	325	194	176	331	396	320	274
radiation	Mo Kα (λ = 710 73 Å)						
abs coeff, cm^{-1}	11.10	10.21	16.58	8.77	5.83	3.41	5.69
T_{max}/T_{min}	1.08	1.08	1.03	1.09	1.04	1.10	1.02
final discrepancy factors							
R	0.0246	0.0407	0.0469	0.0541	0.0616	0.0781	0.0441
R_w	0.0292	0.0448	0.0483	0.0566	0.0761	0.0882	0.0453

for the isolation of VId using the appropriate chelating ligand. Preparations of VIa–c were invariably contaminated by the presence of the tetranuclear species Va–c. Fractional crystallization afforded a convenient method for separation but resulted in poor yields on the order of 5%. Since this class of binuclear complex has been well documented, no further attempts to improve purity and yield were undertaken.

^{17}O NMR Spectra. ^{17}O NMR spectra were recorded at 297 K at 40.66 MHz with use of pulse FT NMR techniques on a Varian XL-300 spectrometer interfaced with a Motorola 6800 microprocessor computer. The spectra were digitized with 6976 data points, depending on the acquisition time and bandwidth employed. The pulse width used for a 90° pulse was 25 μs. Deuterated dichloromethane and acetonitrile were used as internal locks. Spectra were obtained by using a double-precision acquisition technique in cylindrical 10 mm o.d. sample tubes (3.0-mL sample volume) and referenced to internal $H_2{}^{17}O$. Chemical shifts are reported in ppm, with positive values in the low-field direction relative to $H_2{}^{17}O$. All chemical shifts and line width data were reproducible within ±2% and ±5%, respectively.

Spectral Parameters. The following abbreviations are used: cpd, compound; Sol, solvent; [X], molar concentration of X; NT, number of transients; AT, acquisition time in milliseconds, SW, sweep width in hertz; TO, transmitter offset in hertz; LB, exponential line broadening in hertz. The spectral parameters for compounds I, IVa, and Va are presented as follows.

I: cpd, $[Ph_3MeP]_2[Mo_4O_{10}(OCH_3)_6]$; Sol, CD_2Cl_2–CH_3OD (2:1, v/v); [X], 9.3 × 10^{-2}; NT, 70 000; AT, 50; SW, 69 930; TO, 20 000; LB, 30.

IVa: cpd, $[n\text{-}Bu_4N]_2[Mo_4O_{10}(OCH_3)_2(C_6H_4O_2)_2]$; Sol, CD_2Cl_2; [X], 9.3 × 10^{-2}; NT, 99 339; AT, 50; SW, 69 930; TO, 20 000; LB, 25.

Va: cpd, $[n\text{-}Bu_4N]_2[Mo_4O_6(OCH_3)_2(OC_6H_4O)_2(NNC_6H_5)_4]$; Sol, CD_2Cl_2; [X], 9.3 × 10^{-2}; NT, 52 212; AT, 50; SW, 69 930; TO, 20 000; LB, 30.

Thermal Decomposition Studies. Thermal degradation studies of I and IVa were carried out in nitrobenzene at 150 °C. Analysis of the products of the thermal decomposition was performed on a Hewlett-Packard 5890 gas chromatograph/5970 mass spectrometry instrument. The solid residue formed during the thermolysis process was identified as MoO_3 by X-ray powder diffraction. The volatile products were identified as dimethyl ether, methanol, formaldehyde, and water, isolated in the approximate ratio $(CH_3)_2O$:CH_3OH:CH_2O:H_2O of 10:1.5:1.5:1.

X-ray Crystallographic Studies. The details of the crystal data, data collection methods, and refinement procedures for compounds I, II, III, IVa, Vc, Vd, and VId are given in Table I and in Supplementary Table S36. Final positional and thermal parameters, full listings of bond lengths and angles, and hydrogen coordinates of the above complexes are provided in the supplementary material. Full details of crystallographic methodologies may be found in ref 18. All crystals were mounted on the tips of glass fibers and then covered with epoxy resin to protect them from deterioration associated with prolonged exposure to the atmosphere.

Varying degrees of cation disorder were encountered for the structures of IVa, Vc, and Vd. The disorder was adequately modeled by placing carbon atoms at the peak of highest density consistent with an atom position and allowing the positional parameters to vary without constraints. Attempts to assign partial population parameters in the structures of Vc and Vd produced no improvement in the overall residual and resulted in a number of unusual temperature factors. The final difference Fouriers displayed peaks of 1.0 e Å^{-3} in the region of the cations. These were the only significant excursions of electron density on a scale where H atoms exhibited electron densities in the range of 0.8–1.2 e Å^{-3}.

Results and Discussion

Synthesis and Spectroscopic Properties. In methanolic solution, isopolymolybdate anions react to give a variety of oxo–methoxo species of hexavalent molybdenum, of which $[Mo_2O_5(OCH_3)_2]$[15] and $[Mo_8O_{24}(OCH_3)_4]^{4-}$[14] have been previously described. Modification of reaction conditions, most significantly the use of the organic solvent soluble precursor α-$[MePPh_3]_4[Mo_8O_{26}]$,[37] yields the tetranuclear derivative $[MePPh_3]_2[Mo_4O_{10}(OCH_3)_6]$ ($[MePPh_3]_2[I]$) as a pale yellow powder. However, complex I could not be isolated from methanolic solution in the absence of an organic base.

The infrared spectrum of I exhibits absorbances in the 885–930-cm^{-1} region associated with the presence of both terminal and bridging oxo groups and bands at 2900–3000 cm^{-1} assigned to C–H stretching features of the coordinated methoxo groups. Resonances at 946 and 881 ppm in the ^{17}O NMR spectrum of I, illustrated in Figure 2b, confirm the presence of terminal oxo groups in significantly different environments, while the 572 ppm resonance is assigned to a bridging oxo unit, Mo–O–Mo. The crystal structure of I confirms these spectroscopic assignments (vide infra).

Complex I provides a useful precursor for the synthesis of a variety of complexes exhibiting the tetranuclear core and derived from I by substitution of peripheral oxo and/or methoxo groups by suitable ligands. The reaction chemistry of I and its derivatives is illustrated schematically in Figure 1, demonstrating the ubiquitous nature of the tetranuclear core in methanolic solution.

(37) Day, V. W.; Fredrick, M. F.; Klemperer, W. G.; Shum, W. *J. Am. Chem. Soc.* **1977**, *99*, 952.

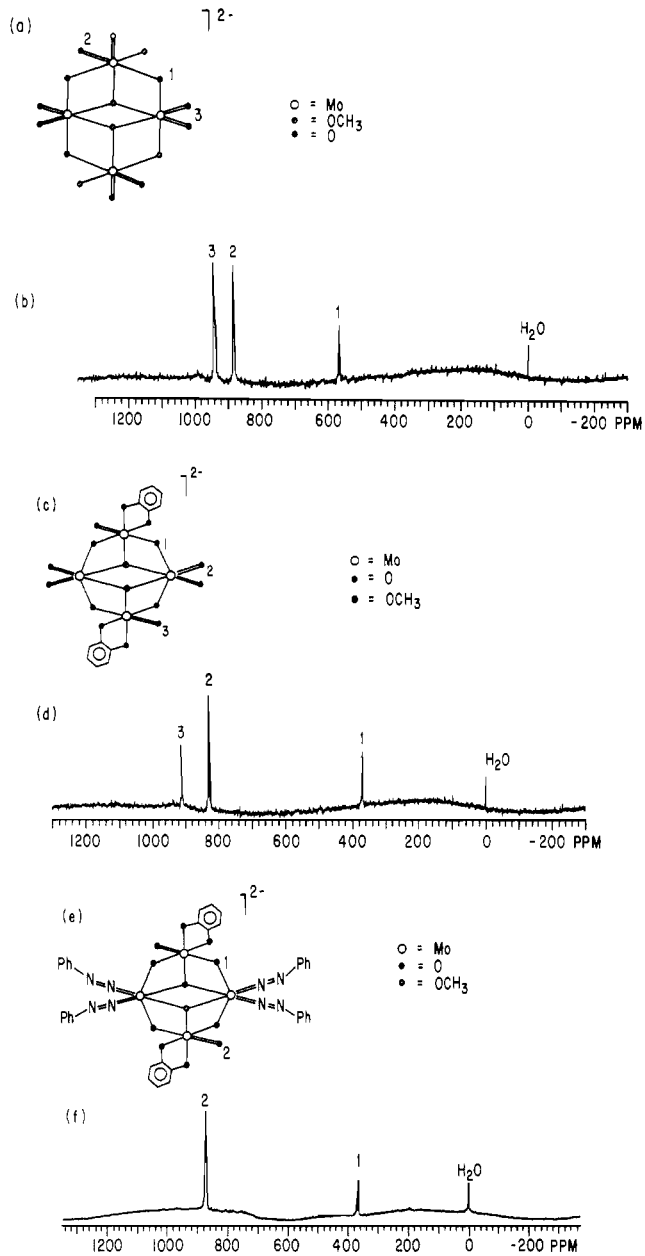

Figure 2. (a) Idealized bond structure of $[Mo_4O_{10}(OCH_3)_6]^{2-}$ (I), with one member from each set of equivalent oxygen atoms labeled. (b) ^{17}O NMR spectrum of I. (c) Idealized bond structure of $[Mo_4O_{10}(OCH_3)_2(OC_6H_4O)_2]^{2-}$ (IVa), with one member from each set of equivalent oxygen atoms labeled. (d) ^{17}O NMR spectrum of IVa. (e) Idealized bond structure of $[Mo_4O_6(OCH_3)_2(OC_6H_4O)_2(NNC_6H_5)_4]^{2-}$ (Va), with one member from each set of equivalent oxygen atoms labeled. (f) ^{17}O NMR spectrum of Va.

Thus, treatment of I with $(CH_3)_3SiCl$ results in displacement of the terminal methoxy groups to give $[n\text{-}Bu_4N]_2[Mo_4O_{10}(OCH_3)_4Cl_2]$ ($[n\text{-}Bu_4N]_2$[II]):

$$[Mo_4O_{10}(OCH_3)_6]^{2-} + 2(CH_3)_3SiCl \rightarrow [Mo_4O_{10}(OCH_3)_4Cl_2]^{2-} + 2(CH_3)_3SiOCH_3$$

Complex II may also be prepared directly from the reaction of α-$[n\text{-}Bu_4N]_4[Mo_8O_{26}]$ with PCl_5. The infrared spectrum of II exhibits features consistent with retention of the core structure and chloride substitution. The 2950–3000-cm^{-1} bands are associated with the C—H stretch of the methoxo units, while the 912- and 940-cm^{-1} features may be assigned to ν_{as}(Mo=O) and ν_s(Mo=O), respectively. The bridging oxo group gives rise to the strong band at 895 cm^{-1}, while the 450-cm^{-1} feature reveals the presence of the Mo—Cl unit. The ^{17}O NMR spectrum is nearly identical with that of I, strongly suggesting retention of the tetranuclear core, an observation confirmed in the structural studies.

Reaction of complex II with thiolate ligands resulted in reduction of the cluster to a mixed-valence Mo(VI)/Mo(V) polyoxochloromolybdate, $[Et_3NH]_2[Mo_4O_8(OCH_3)_4Cl_4]$ ($[Et_3NH]_2$[III]), which crystallizes as a Chinese red diamagnetic species. The infrared spectrum of III displays a feature at 2980 cm^{-1} attributed to the C—H stretch of the methoxo groups, while the strong bands at 960 and 940 cm^{-1} are assigned to ν(Mo=O) for two structurally distinct Mo–terminal oxo group units. The bands at 795 and 725 cm^{-1} are assigned to the doubly and triply bridging oxo groups, (MoOMo) and (Mo_3O), respectively, and the 490-cm^{-1} feature is assigned to the Mo–Cl stretch. The electronic spectrum of III exhibits a single transition at 317 nm ($\epsilon = 3.5 \times 10^3$ M^{-1} cm^{-1}) assigned as a ligand to metal charge-transfer band. No bands attributable to intervalence charge transfer were observed at low energy.[38,39] The observation of an unperturbed ^1H NMR spectrum at 22 °C reveals no evidence for valence trapping at this temperature. EPR spectra of frozen solutions (77 K) of III displayed poorly resolved, weak signals from which no conclusions were drawn regarding the localization of sites, $[Mo^V_2Mo^{VI}_2O_8(OCH_3)_4Cl_4]^{2-}$.

Reactions of I with a variety of catecholates yield complexes of the general class $[Mo_4O_{10}(OCH_3)_2(LL)_2]^{2-}$, where LL = catecholate, 3-*tert*-butylcatecholate, and 2,3-dihydroxynaphthalene. Alternatively, and more conveniently, direct reactions of α-$[n\text{-}Bu_4N]_4[Mo_8O_{26}]$ with the appropriate ligand yield the complexes $[n\text{-}Bu_4N]_2[Mo_4O_{10}(OCH_3)_2(LL_2)_2]$ (LL = catecholate, $(C_6H_4O_2)^{2-}$ ($[n\text{-}Bu_4N]_2$[IVa]); LL = 3-*tert*-butylcatecholate, $(Bu^tC_6H_3O_2)^{2-}$ ($[n\text{-}Bu_4N]_2$[IVb]); LL = naphthalene-2,3-diolate, $(C_{10}H_6O_2)^{2-}$ ($[n\text{-}Bu_4N]_2$[IVc]); LL = *o*-aminophenolate, (OC_6H_4NH) ($[n\text{-}Bu_4N]_2$[IVd]). The infrared spectrum of IVa is characteristic for the series IVa–d and displays the features consistent with the methoxooxomolybdate tetranuclear core: a strong band at 2960 cm^{-1}, assigned to the C—H stretch of the methoxo groups, the 935- and 910-cm^{-1} absorptions associated with molybdenum–terminal oxo group interactions, and a feature at 730 cm^{-1} due to the bridging oxo group. The complexes IVa–d are diamagnetic, emerald green or green/black, crystalline solids. The electronic spectra exhibit transitions in the 265–285-nm range tentatively assigned to ligand to metal charge-transfer bands (ϵ = ca. 10^3–10^4 cm^{-1} M^{-1}). The ^{17}O NMR spectrum of IVa reveals features consistent with the presence of both bridging and terminal oxo groups, as shown in Figure 2d. The single resonance at 373 ppm is well within the range associated with doubly bridging oxo groups, O1 type (250–520 ppm),[40] confirming that the bridging oxo groups are equivalent. The transitions at 829 and 912 ppm lie within the range characteristic for Mo(VI)–terminal oxo groups.[41] The linear correlation that exists between Mo–O π-bond order and ^{17}O chemical shift has been interpreted in terms of increasing π-bond order augmenting the paramagnetic screening of the oxygen nucleus, resulting in a larger chemical shift relative to that of $H_2{}^{17}O$.[41] Whereas oxygen atoms of type O2 must compete for the Mo t_{2g} type orbitals for the π-electron density, the O3 type terminal oxo group is bonded to the Mo center possessing no other terminal oxo group and may be anticipated to participate more effectively in π-bonding, shifting the resonance downfield to 912 ppm. Although intensities of ^{17}O NMR resonances provide only a qualitative measure of the relative number of oxygen nuclei, the relative peak heights of the resonances at 829 and 912 ppm for IVa support the assignments of these resonances to O2 and O3, respectively.

Complexes IVa–d react with phenylhydrazine in methanol solution to yield the deep purple crystalline complexes of the class $[n\text{-}Bu_4N]_2[Mo_4O_6(OCH_3)_2(NNC_6H_5)_4(LL)_2]$ (LL = catecholate, $(OC_6H_4O)^{2-}$ ($[n\text{-}Bu_4N]_2$[Va]); LL = 3-*tert*-butylcatecholate, $(Bu^tC_6H_3O_2)^{2-}$ ($[n\text{-}Bu_4N]_2$[Vb]); LL = naphthalene-2,3-diolate, $(C_{10}H_6O_2)^{2-}$ ($[n\text{-}Bu_4N]_2$[Vc]); LL = *o*-aminophenolate,

(38) Robin, M. B.; Day, P. *Adv. Inorg. Chem. Radiochem.* **1967**, *10*, 247.
(39) Varga, G. M., Jr.; Papaconstantinou, E.; Pope, M. T. *Inorg. Chem.* **1970**, *9*, 662.
(40) Klemperer, W. G. *Angew. Chem., Int. Ed. Engl.* **1978**, *17*, 246.
(41) Kidd, R. G. *Can. J. Chem.* **1967**, *45*, 605.

$(OC_6H_4NH)^{2-}$ ($[n\text{-}Bu_4N]_2[Vd]$)). The syntheses exploit the condensation type reaction

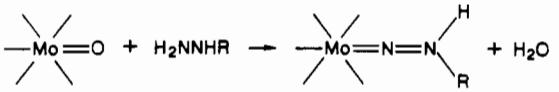

characteristic of the chemistry of phenylhydrazine with metal–oxo complexes, although the fate of the N-terminal hydrogen has yet to be established.[25] The complexes Va–d were alternatively prepared from the reaction of $[n\text{-}Bu_4N]_2[Mo_4O_8(OCH_3)_2(NNC_6H_5)_4]$[25] with the appropriate ligand LLH_2. The infrared spectrum of Vc is characteristic of this series, exhibiting the usual pattern of absorbances associated with the methoxooxomolybdate tetranuclear core: the 2960-cm^{-1} band associated with the C—H stretch of the bridging $-OCH_3$ group, the 940- and 890-cm^{-1} absorptions assigned to ν_s(Mo=O) and ν_{as}(Mo=O), respectively, and the 765-cm^{-1} band from the bridging oxo moiety. In addition, the medium-strong absorptions at 1570 and 1510 cm^{-1}, assigned to ν_s(N=N) and ν_{as}(N=N), confirm the presence of the *cis*-bis(diazenido)molybdenum unit. Furthermore, the electronic spectra of Va–d exhibit a transition at ca. 500–520 nm characteristic for ligand to metal charge transfer of the $[Mo(NNC_6H_5)_2]^{2+}$ functional unit. An unusual feature of these complexes is the oxidation state formalism that results if the diazenido ligands are considered the monopositive, three-electron donors $(NNR)^+$ in analogy to the isoelectronic nitrosyl ligand NO.[42] The diazenido-coordinated Mo centers are the formally Mo(0) moieties, and complexes Va–d may be considered mixed-valence complexes of Mo(VI) and Mo(0).

The ^{17}O spectrum of Va, illustrated in Figure 2f, exhibits resonances at 873 and 368 ppm, attributed to the terminal oxo groups of five-coordinate Mo centers and the bridging oxo groups, respectively. Substitution of diazenido ligands in Va for the two pairs of *cis*-dioxo groups of IVa has resulted in the disappearance of the transition of 912 ppm associated with the *cis*-dioxo groups.

In contrast to the preparations of Va–d, the reactions of $[n\text{-}Bu_4N]_2[Mo_4O_8(OCH_3)_2(NNC_6H_5)_4]$ with excess ligand of the catechol type yield binuclear complexes of the general class $[Mo_2(OCH_3)_2(NNC_6H_5)_4(LL)_2]^{2-}$ (VIa–c). With *o*-aminophenol, the neutral complex $[Mo_2(OCH_3)_2(NNC_6H_5)_4(OC_6H_4NH_2)_2]\cdot 2DMF$ (VId) was isolated as black diamagnetic crystals in good yield. The infrared spectrum of VId confirms the absence of both bridging and terminal oxo groups but exhibits characteristic features in the 1600–1670-cm^{-1} range associated with the *cis*-bis(diazenido)molybdate unit. The charge-transfer band at 519 nm in the electronic spectrum of VId confirms the presence of the $[Mo(NNC_6H_5)_2]^{2+}$ unit.

Thermal and photochemical decomposition studies of complexes of the types V and VI yield intractable mixtures of amorphous solids. On the other hand, complexes I and IVa yield identifiable products, although the thermal decomposition characteristics display significant contrasts. While the thermal decomposition of I at 150 °C yields dimethyl ether, formaldehyde, methanol, and water as products, the decomposition of IVa produces only water and methanol as volatile products. This result is consistent with the presence of significant intramolecuar C–H···O contacts in I, providing a mechanism for C–H bond activation,[14-16,43] and with the absence of close C–H···O contacts in IVa. These observations are consistent with models proposed for C–H bond activation in the oxidation of methanol to formaldehyde.[14-16,43]

Description of the Structures. The structures of the $[Mo_4O_{10}(OCH_3)_6]^{2-}$ complex anion I is displayed in Figure 3. The overall cluster geometry is similar to that described for the neutral tetramolybdate $[Mo_4O_8(OC_2H_5)_2(CH_3C(CH_2O)_3)_2]$[17] and is closely related to the "$[Mo_4O_{13}]^{2-n}$" asymmetric unit common to the $[(X)_2Mo_8O_{26}]^{2n-4}$ clusters and to their parent structure β-$[Mo_8O_{26}]^{4-}$.[44] This structural relationship is schematically illustrated in Figure 4, an idealized representation of the structures as edge-sharing octahedra. Structures II, III, and VIa are also presented to illustrate the persistence of the general tetranuclear core.

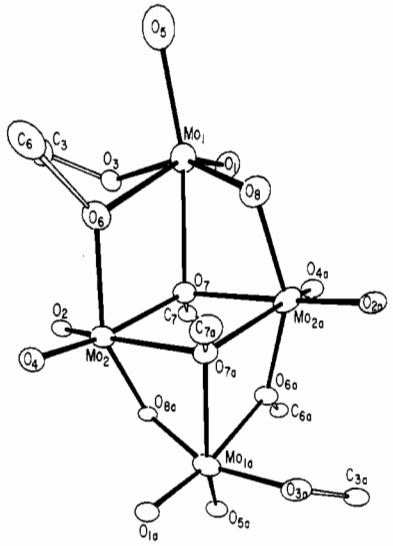

Figure 3. ORTEP view of the structure of $[Mo_4O_{10}(OCH_3)_6]^{2-}$ (I), showing the atom-labeling scheme.

Table II. Atomic Positional Parameters ($\times 10^4$) and Temperature Factors ($Å^2 \times 10^3$) for $[Ph_3PMe]_2[Mo_4O_{10}(OCH_3)_6]$ ($[Ph_3PMe]_2[I]$)

atom	x	y	z	U_{iso}[a]
Mo1	−2459 (1)	285 (1)	−2989 (1)	27 (1)
Mo2	−4338 (1)	−990 (1)	−5994 (1)	25 (1)
P1	2427 (1)	2609 (1)	9317 (1)	29 (1)
O1	−1950 (2)	1803 (2)	−2429 (2)	42 (1)
O2	−2958 (2)	−734 (2)	−6534 (2)	38 (1)
O3	−999 (2)	227 (2)	−3705 (2)	35 (1)
O4	−5001 (2)	−2518 (2)	−6407 (2)	39 (1)
O5	−1867 (2)	−607 (2)	−1824 (2)	43 (1)
O6	−3419 (2)	−1402 (2)	−4288 (2)	29 (1)
O7	−3757 (2)	771 (2)	−4801 (2)	25 (1)
O8	−4392 (2)	151 (2)	−2935 (2)	29 (1)
C3	−381 (3)	−837 (3)	−3874 (4)	46 (1)
C6	−3428 (4)	−2630 (3)	−3893 (3)	48 (1)
C7	−3208 (3)	1828 (3)	−5288 (3)	36 (1)
C10	4204 (3)	2330 (3)	9840 (3)	29 (1)
C11	4618 (3)	1662 (3)	10842 (3)	36 (1)
C12	5937 (3)	1340 (3)	11197 (3)	40 (1)
C13	6849 (3)	1693 (3)	10564 (3)	42 (1)
C14	6445 (3)	2333 (3)	9560 (3)	42 (1)
C15	5115 (3)	2657 (3)	9181 (3)	35 (1)
C16	2000 (3)	3479 (3)	10476 (3)	32 (1)
C17	2973 (3)	4336 (3)	11270 (3)	40 (1)
C18	2593 (4)	5073 (3)	12098 (3)	53 (1)
C19	1244 (4)	4935 (3)	12110 (4)	57 (2)
C20	296 (4)	4070 (4)	11339 (4)	69 (2)
C21	641 (4)	3338 (3)	10500 (4)	52 (1)
C22	2172 (3)	3506 (3)	8030 (3)	32 (1)
C23	2865 (4)	4718 (3)	8175 (3)	44 (1)
C24	2707 (4)	5404 (3)	7183 (4)	55 (2)
C25	1875 (4)	4923 (3)	6085 (4)	59 (2)
C26	1141 (4)	3726 (3)	5936 (3)	59 (2)
C27	1308 (3)	3002 (3)	6911 (3)	43 (1)
C28	1352 (3)	1152 (3)	8934 (3)	40 (1)

[a] Equivalent isotropic U defined as one-third of the trace of the orthogonalized U_{iso} tensor.

The Mo centers of I display $[MoO_6]$ pseudooctahedral geometries through coordination to oxo and methoxo ligands. The cluster is located at the crystallographic center of symmetry, relating the crystallographically independent $[Mo_2O_4(\mu\text{-}O)(OCH_3)(\mu_3\text{-}OCH_3)_2]$ units. A unique feature of the structure is the presence of terminal and doubly and triply bridging methoxo groups. Both molybdenum centers exhibit the typical two short–two intermediate–two long Mo–O distorted-octahedral

(42) Sutton, D. *Chem. Soc. Rev.* **1975**, *4*, 443. Ibers, J. A.; Haymore, B. L. *Inorg. Chem.* **1975**, *14*, 1369.
(43) Anderson, A. B.; Ray, N. K. *J. Am. Chem. Soc.* **1985**, *107*, 253.
(44) Lindquist, I. *Ark. Kemi* **1950**, *2*, 349. Atovmyan, L. O.; Krasochke, O. N. *J. Struct. Chem. (Engl. Transl.)* **1972**, *13*, 319.

Table III. Selected Bond Lengths (Å) and Angles (deg) for $[Ph_3MeP]_2[Mo_4O_{10}(OCH_3)_6]$ ($[Ph_3PMe]_2[I]$)

Mo1–O1	1.707 (2)	Mo2–O2	1.703 (2)
Mo1–O3	1.915 (2)	Mo2–O4	1.705 (2)
Mo1–O5	1.710 (2)	Mo2–O6	2.032 (2)
Mo1–O6	2.249 (2)	Mo2–O7	2.225 (2)
Mo1–O7	2.263 (2)	Mo2–O7a	2.416 (2)
Mo1–O8	1.977 (2)	Mo2–O8a	1.869 (2)
Mo1···Mo2	3.589 (1)	Mo2···Mo2a	3.731 (1)
Mo1···Mo2a	3.320 (1)		
O1–Mo1–O6	160.8 (1)	O2–Mo2–O7a	165.1 (1)
O3–Mo1–O8	156.8 (1)	O4–Mo1–O7	155.9 (1)
O5–Mo1–O7	158.3 (1)	O6–Mo2–O8a	149.8 (1)
O1–Mo1–O5	106.8 (1)	O2–Mo2–O4	105.4 (1)
O1–Mo1–O3	94.6 (1)	O2–Mo2–O6	101.9 (1)
O1–Mo1–O7	93.9 (1)	O2–Mo2–O7	94.3 (1)
O1–Mo1–O8	97.8 (1)	O2–Mo2–O8	100.2 (1)
O3–Mo1–O5	98.6 (1)	O4–Mo2–O6	90.6 (1)
O3–Mo1–O6	82.0 (1)	O4–Mo2–O7a	88.8 (1)
O3–Mo1–O7	86.2 (1)	O4–Mo2–O8a	103.1 (1)
O5–Mo1–O6	92.4 (1)	O6–Mo2–O7	71.6 (1)

Table IV. Atomic Positional Parameters ($\times 10^4$) and Temperature Factors ($Å^2 \times 10^3$) for $[n\text{-}Bu_4N]_2[Mo_4O_{10}(OCH_3)_4Cl_2]$ ($[n\text{-}Bu_4N]_2[II]$)

atom	x	y	z	U_{eq}[a]
Mo1	1119 (1)	1577 (1)	2430 (1)	41 (1)
Mo2	−95 (1)	−1495 (1)	216 (1)	37 (1)
Cl1	113 (2)	392 (2)	3326 (2)	61 (1)
O1	−694 (4)	308 (3)	749 (3)	35 (2)
O2	1558 (4)	−247 (4)	1606 (3)	43 (2)
O3	1566 (4)	1908 (3)	1230 (3)	40 (2)
O4	229 (5)	2683 (4)	2786 (4)	60 (2)
O5	2734 (5)	2141 (4)	3483 (4)	64 (2)
O6	964 (5)	−2459 (4)	−135 (4)	59 (2)
O7	−991 (5)	−2146 (4)	857 (4)	55 (2)
N1	594 (5)	3799 (4)	6893 (4)	40 (2)
C1	−2158 (7)	199 (6)	675 (6)	53 (3)
C2	2699 (8)	−647 (7)	2210 (7)	75 (4)
C11	1642 (7)	5060 (5)	7391 (5)	45 (3)
C12	2685 (7)	5439 (6)	8596 (6)	53 (3)
C13	3768 (8)	6630 (7)	8928 (7)	70 (4)
C14	4762 (9)	7159 (8)	10186 (8)	88 (5)
C15	−294 (7)	3765 (6)	7628 (6)	47 (3)
C16	−1275 (7)	4642 (6)	7696 (6)	50 (3)
C17	−2045 (8)	4535 (8)	8484 (7)	67 (4)
C18	−3257 (8)	5165 (7)	8440 (7)	67 (4)
C19	−336 (7)	3611 (6)	5675 (6)	49 (3)
C20	−1581 (8)	2500 (7)	5048 (6)	57 (3)
C21	−2446 (8)	2502 (8)	3894 (7)	70 (4)
C22	−3741 (10)	1505 (9)	3240 (8)	92 (5)
C23	1360 (7)	2748 (5)	6864 (6)	46 (3)
C24	2481 (7)	2712 (6)	6335 (5)	47 (3)
C25	3102 (8)	1604 (7)	6357 (7)	62 (4)
C26	4327 (9)	1541 (9)	5913 (7)	81 (5)

[a] Equivalent isotropic U defined as one-third of the trace of the orthogonalized U_{eq} tensor.

coordination observed in isopolymolybdates and molybdenum(VI) oxide systems,[45] as shown in Table III.

Complex II, shown in Figure 5, is derived from I by substitution of the two terminal methoxo groups by chloro ligands. The tetranuclear cluster is situated on a center of symmetry, presenting two crystallographically unique pseudooctahedral Mo centers. The Mo2 site displays a $[MoO_6]$ geometry through ligation to two terminal and one bridging oxo groups and two triply bridging and one doubly bridging methoxo group, while the Mo1 center enjoys $[MoO_5Cl]$ coordination to one doubly bridging and one triply bridging methoxy group, one bridging and two terminal oxo groups, and the terminal chloride ligand. The structural parameters listed in Table V are nearly identical with those for I, indicating that substitution of peripheral cluster ligands produces no dramatic structural changes in the tetranuclear core. The

(45) Kihlborg, L. *Ark. Kemi* **1963**, *21*, 357.

Table V. Selected Bond Lengths (Å) and Angles (deg) for $[n\text{-}Bu_4N]_2[Mo_4O_{10}(OCH_3)_4Cl_2]$ ($[n\text{-}Bu_4N]_2[II]$)

Mo1–Cl1	2.416 (2)	Mo2–O1	2.218 (4)
Mo1–O1	2.286 (3)	Mo2–O1a	2.389 (5)
Mo1–O2	2.222 (4)	Mo2–O2	2.026 (3)
Mo1–O3	1.911 (5)	Mo2–O3a	1.901 (4)
Mo1–O4	1.691 (6)	Mo2–O6	1.704 (5)
Mo1–O5	1.682 (4)	Mo2–O7	1.687 (6)
Mo1···Mo2	3.577 (1)	Mo2···Mo2a	3.724 (1)
Mo1···Mo2a	3.290 (1)		
Cl1–Mo1–O3	157.7 (1)	O1–Mo2–O6	156.2 (2)
O1–Mo1–O5	161.0 (2)	O1a–Mo2–O7	165.3 (2)
O2–Mo1–O4	161.0 (2)	O2–Mo2–O3a	150.6 (2)
O1–Mo1–O2	67.4 (1)	O1–Mo2–O1a	72.2 (2)
O1–Mo1–O3	74.3 (2)	O1–Mo2–O2	72.1 (2)
O1–Mo1–O4	94.8 (2)	O1–Mo2–O3a	85.7 (2)
O1–Mo1–Cl1	86.0 (1)	O1–Mo2–O7	95.4 (2)
O2–Mo1–O3	82.3 (2)	O1a–Mo2–O2	82.8 (2)
O2–Mo1–O5	93.4 (2)	O1a–Mo2–O3a	71.9 (2)
O3–Mo1–Cl1	80.5 (1)	O1a–Mo2–O6	89.0 (2)

Table VI. Atomic Coordinates ($\times 10^4$) and Equivalent Isotropic Temperature Factors ($Å^2 \times 10^3$) for $[Et_3NH]_2[Mo_4O_8(OCH_3)_4Cl_4]$ ($[Et_3NH]_2[III]$)

atom	x	y	z	U_{eq}[a]
Mo1	622 (1)	4275 (1)	9109 (1)	35 (1)
Mo2	−1123 (1)	3290 (1)	9917 (1)	36 (1)
Cl1	682 (2)	4979 (2)	7313 (1)	57 (1)
Cl2	−3230 (2)	2663 (2)	9258 (2)	59 (1)
O1	246 (4)	4202 (3)	10581 (3)	36 (1)
O2	1669 (5)	3348 (4)	9000 (4)	53 (2)
O3	−1036 (4)	3781 (4)	8497 (3)	41 (1)
O4	−2067 (4)	4663 (4)	10354 (4)	42 (2)
O5	−452 (5)	2136 (4)	9998 (5)	57 (2)
O6	−1508 (7)	3025 (5)	11577 (4)	69 (2)
C1	−3320 (7)	4788 (7)	10574 (8)	71 (4)
C2	−1667 (16)	2188 (9)	12164 (10)	123 (7)
N1	2717 (7)	931 (5)	1395 (5)	51 (2)
C3	2773 (9)	2053 (7)	1208 (7)	62 (3)
C4	4036 (11)	2399 (9)	911 (9)	91 (5)
C5	1537 (9)	670 (7)	1834 (7)	64 (3)
C6	1568 (12)	−398 (8)	2268 (9)	95 (5)
C7	2939 (9)	303 (7)	445 (7)	67 (3)
C8	1911 (9)	468 (9)	−512 (7)	81 (4)

[a] Equivalent isotrpic U defined as one-third of the trace of the orthogonalized U_{ij} tensor.

Table VII. Selected Bond Lengths (Å) and Angles (deg) for $[Et_3NH]_2[Mo_4O_8(OCH_3)_4Cl_4]$ ($[Et_3NH]_2[III]$)

Mo1–Cl1	2.472 (2)	Mo2–Cl2	2.427 (2)
Mo1–O1	1.970 (4)	Mo2–O1	1.984 (4)
Mo1–O2	1.673 (5)	Mo2–O3	1.931 (4)
Mo1–O3	1.939 (4)	Mo2–O4	2.180 (5)
Mo1–O1a	2.267 (5)	Mo2–O5	1.678 (5)
Mo1–O4a	2.121 (4)	Mo2–O6	2.232 (5)
Mo1–Mo2	2.595 (1)	Mo1···Mo1a	3.373 (1)
		Mo1···Mo2a	3.454 (1)
Cl1–Mo1–O1	158.5 (1)	Cl2–Mo2–O1	160.3 (1)
	95.4 (2)	O4–Mo2–O5	160.9 (2)
Cl1–Mo1–O2	84.1 (1)	O3–Mo2–O6	167.1 (2)
Cl1–Mo1–O3	93.9 (2)	Cl2–Mo2–O3	87.5 (1)
O1–Mo1–O3	107.5 (2)	O1–Mo2–O3	93.7 (2)
O2–Mo1–O3		O5–Mo2–O3	106.5 (2)

structural analogy of I and II is adequately represented by the polyhedron models of the structures shown in Figure 4.

The structure of the reduced cluster $[n\text{-}Bu_4N]_2[Mo_4O_8(OCH_3)_4Cl_4]$ ($[n\text{-}Bu_4N]_2[III]$) is illustrated in Figure 6, and selected metrical parameters are presented in Table VII. The tetranuclear cluster dianion is located on a crystallographic center of symmetry, with the unique molybdenum centers displaying $[MoO_5Cl]$ coordination geometries. The Mo1 center exhibits ligation to one terminal, one doubly bridging, and two triply bridging oxo groups, one bridging methoxo group, and a terminal

Table VIII. Comparison of Structural Parameters (Å) for Selected Polyoxomolybdate–Alkoxide and Polyoxomolybdate–Alkoxide–Chloride Complexes

	$[Mo_8O_{24}(OCH_3)_4]^{4-}$	$[Mo_4O_{10}(OCH_3)_2(OC_6H_4O)_2]^{2-}$	$[Mo_4O_{10}(OCH_3)_6]^{2-}$	$[Mo_4O_{10}(OCH_3)_4Cl_2]^{2-}$	$[Mo_4O_8(OCH_3)_4Cl_4]^{2-}$	$[Mo_4O_6(n\text{-}OC_3H_7)_6Cl_4]$
Mo–O_t	1.711 (6)	1.686 (16)	1.707 (5)	1.696 (8)	1.676 (6)	1.63 (2)
Mo–(μ-O)	1.948 (2), 1.929 (2)	1.9877 (11), 1.821 (10)	1.978 (2), 1.872 (2)	1.911 (5), 1.901 (5)	1.939 (4), 1.931 (4)	
Mo–(μ_3-O)	1.918–2.260 (4)				1.970–2.267 (5)	1.96–2.34 (1)
Mo–OR	1.909 (2)	1.982 (10)	1.922 (2)		2.232 (5)	2.13 (1)
Mo–(μ-OR)	2.261 (2), 1.995 (2)		2.249 (2), 2.035 (2)	2.226 (5), 2.029 (5)	2.180 (5), 2.121 (4)	2.09 (2), 1.98 (1)
Mo–(μ_3-OR)		2.248–2.416 (7)	2.228–2.417 (2)	2.218–2.389 (6)		
Mo–Cl				2.416 (2)	2.450 (3)	2.38 (1)
ref	14	18, this work	18, this work	this work	35, this work	36

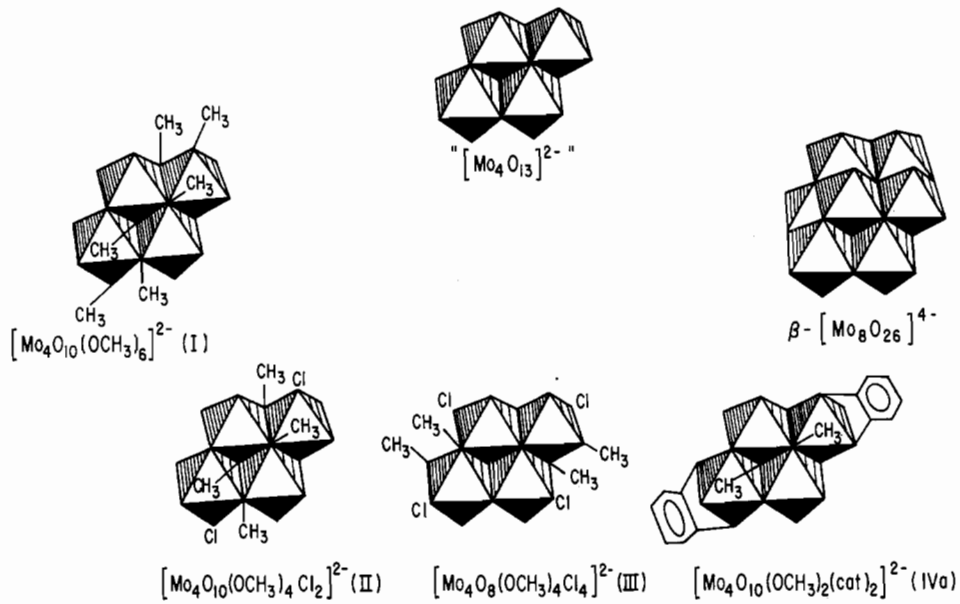

Figure 4. Idealized polyhedral models illustrating the structural relationship of the "$[Mo_4O_{13}]^{2-n}$" asymmetric unit, β-$[Mo_8O_{26}]^{4-}$, $[Mo_4O_{10}(OCH_3)_6]^{2-}$ (I), $[Mo_4O_{10}(OCH_3)_4Cl_2]^{2-}$ (II), $[Mo_4O_8(OCH_3)_4Cl_4]^{2-}$ (III), and $[Mo_4O_{10}(OCH_3)_2(OC_6H_4O)_2]^{2-}$ (IVa).

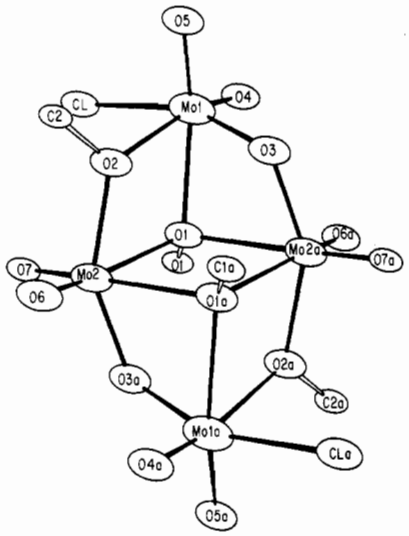

Figure 5. Perspective view of the structure of $[Mo_4O_{10}(OCH_3)_4Cl_2]^{2-}$ (II), showing the atom-labeling scheme.

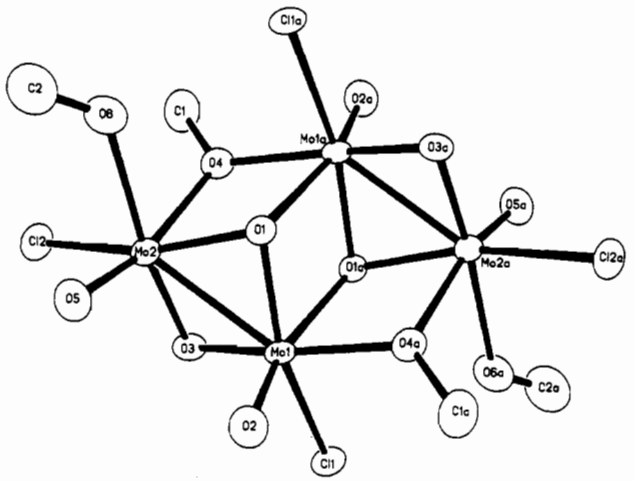

Figure 6. Perspective view of the structure of $[Mo_4O_8(OCH_3)_4Cl_4]^{2-}$ (III), showing the atom-labeling scheme.

chloride ligand, while the Mo2 center bonds to one terminal, one doubly bridging, and a single triply bridging oxo group, one terminal and one bridging methoxo group, and a terminal chloride donor. A major consequence of cluster reduction is the shortening of the Mo1–Mo2 distance to 2.595 (1) Å, a bond length consistent with a significant degree of metal–metal bonding. A comparison of the structural parameters of III with those of other oxoalkoxopolymolybdates chloropolymolybdates, presented in Table VIII, reveals a number of persistent features associated with the core geometries. The molybdenum bond distances to terminal oxo groups, terminal chloride donors, and triply bridging oxo groups exhibit uniform patterns for the class of structures. In contrast, the Mo–terminal methoxo oxygen distance associated with III is significantly longer than this distance for polymolybdate(VI) clusters (2.232 vs 1.95 Å) and even for the Mo(VI/Mo(V) species $[Mo_4O_6(OR)_6Cl_4]$ (2.13 Å).[36] Furthermore, the doubly bridging methoxo group of III presents Mo–O bond distances, 2.180 (5) and 2.121 (4) Å, significantly more symmetrical than those associated with the fully oxidized clusters, ca. 2.245 and 2.020 Å. The pronounced long–short alternation of these bonds is a characteristic feature of the alkoxopolymolybdate cores of all other examples presented herein and studied to date.

As shown schematically in Figure 7, II is an example of a class of tetranuclear oxoalkoxochloromolybdates structurally related

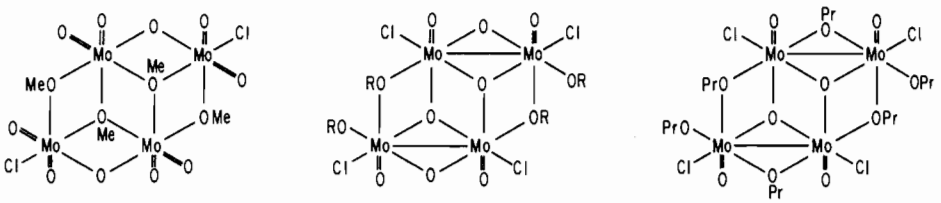

$[Mo_4O_{10}(OMe)_4Cl_2]^{2-}$ $[Mo_4O_8(OR)_4Cl_4]^{2-}$ R = -Me, -Et $[Mo_4O_6(OPr)_6Cl_4]$

Figure 7. Schematic representation of the structures of the class of tetranuclear oxoalkoxochloromolybdates $[Mo_4O_{10}(OCH_3)_4Cl_2]^{2-}$ (II), $[Mo_4O_8(OCH_3)_4Cl_4]^{2-}$ (III), and $[Mo_4O_6(n\text{-}OC_3H_7)_6Cl_4]$.

Table IX. Atom Coordinates ($\times 10^4$) and Temperature Factors ($Å^2 \times 10^3$) for $[Bu_4N]_2[Mo_4O_{10}(OCH_3)_2(OC_6H_4O)_2]$ ($[Bu_4N]_2$[IVa])

atom	x	y	z	U_{iso}[a]	atom	x	y	z	U_{iso}[a]
Mo1	-172 (1)	6358 (1)	4158 (1)	44 (1)*	N1	7958 (6)	2738 (7)	1038 (6)	68 (5)*
Mo2	950 (1)	4795 (1)	4888 (1)	45 (1)*	N2	2435 (6)	7037 (7)	4173 (5)	64 (5)*
Mo3	3680 (1)	5086 (1)	365 (1)	45 (1)*	C15	8733 (8)	2461 (9)	1442 (7)	77 (5)
Mo4	5156 (1)	3932 (1)	332 (1)	49 (1)*	C16	9338 (10)	3156 (11)	1695 (9)	106 (6)
O1	-316 (4)	4906 (4)	4359 (4)	40 (3)*	C17	10011 (10)	2800 (11)	2286 (9)	116 (7)
O2	5036 (4)	5253 (4)	600 (4)	40 (3)*	C18	10569 (14)	3411 (16)	2489 (12)	180 (11)
O3	1119 (5)	4461 (6)	4167 (5)	74 (5)*	C19	7616 (9)	3319 (9)	1458 (7)	75 (5)
O4	1813 (5)	4925 (6)	5454 (5)	75 (4)*	C20	7562 (9)	3022 (9)	2129 (7)	85 (5)
O5	1 (5)	7389 (5)	4156 (4)	64 (4)*	C21	7222 (10)	3704 (10)	2471 (8)	92 (5)
O6	758 (4)	5978 (5)	4650 (4)	46 (3)*	C22	7163 (12)	3466 (14)	3155 (11)	154 (9)
O7	-672 (4)	6293 (5)	4802 (4)	51 (4)*	C23	7482 (8)	1928 (9)	869 (8)	75 (5)
O8	90 (5)	6013 (5)	3326 (4)	57 (4)*	C24	6649 (10)	2033 (11)	473 (9)	108 (6)
O9	-1178 (4)	6260 (5)	3456 (4)	53 (4)*	C25	6274 (11)	1182 (12)	414 (11)	140 (8)
O10	5070 (5)	3072 (5)	-160 (5)	71 (4)*	C26	5525 (15)	1157 (18)	174 (15)	246 (15)
O11	5418 (5)	3609 (6)	1155 (5)	76 (4)*	C27	7951 (9)	3195 (9)	389 (7)	83 (5)
O12	2730 (4)	4911 (5)	91 (5)	61 (4)*	C28	8229 (10)	2742 (10)	-137 (8)	94 (5)
O13	4063 (4)	4084 (4)	185 (4)	48 (3)*	C29	8264 (11)	3307 (11)	-708 (9)	110 (6)
O14	6185 (4)	4298 (5)	344 (4)	50 (3)*	C30	8435 (12)	2861 (12)	-1280 (10)	144 (8)
O15	3719 (5)	6140 (5)	868 (4)	55 (4)*	C31	2269 (8)	7725 (10)	3640 (7)	83 (5)
O16	3956 (5)	4716 (5)	1347 (4)	64 (4)*	C32	1417 (10)	7826 (11)	3274 (9)	105 (6)
C1	-667 (7)	4322 (8)	3814 (6)	58 (4)	C33	1247 (12)	8557 (12)	2832 (10)	131 (7)
C2	5537 (7)	5552 (8)	1231 (6)	64 (4)	C34	1426 (11)	9335 (11)	3192 (10)	134 (8)
C3	-506 (7)	5911 (8)	2741 (7)	58 (4)	C35	2088 (8)	6222 (8)	3851 (7)	70 (4)
C4	-408 (10)	5661 (10)	2113 (8)	88 (5)	C36	2368 (10)	5915 (11)	3267 (8)	93 (5)
C5	-1084 (9)	5572 (10)	1570 (8)	94 (5)	C37	1920 (12)	5206 (13)	2900 (11)	140 (8)
C6	-1767 (10)	5705 (10)	1647 (8)	95 (5)	C38	2205 (13)	4845 (14)	2338 (11)	161 (9)
C7	-1858 (9)	5958 (9)	2279 (7)	75 (4)	C39	3279 (8)	6964 (9)	4429 (7)	74 (4)
C8	-1183 (7)	6033 (8)	2817 (7)	57 (4)	C40	3544 (10)	6303 (11)	4973 (9)	106 (6)
C9	3889 (8)	6104 (9)	1549 (7)	68 (4)	C41	4422 (13)	6238 (15)	5250 (12)	156 (9)
C10	3938 (8)	6803 (10)	1964 (7)	78 (5)	C42	4652 (23)	6492 (25)	5801 (18)	436 (32)
C11	4126 (9)	6632 (10)	2674 (8)	88 (5)	C43	2091 (8)	7204 (9)	4727 (7)	75 (4)
C12	4275 (9)	5889 (10)	2934 (8)	87 (5)	C44	2379 (10)	7983 (11)	5148 (9)	107 (6)
C13	4230 (9)	5169 (10)	2530 (8)	87 (5)	C45	1776 (16)	8217 (18)	5537 (15)	195 (12)
C14	4032 (8)	5333 (8)	1823 (7)	61 (4)	C46	1854 (30)	8790 (28)	5784 (26)	603 (59)

[a] Values marked with an asterisk denote equivalent isotropic U values, defined as one-third of the trace of the orthogonalized U_{iso} tensor.

by the tetranuclear core of edge-sharing octahedra $[MoO_5X]$, where X = O, Cl. Considerable variation in the nature of peripheral ligands, the terminal and doubly bridging groups, is observed. However, the central core consists of a $[Mo_4(\mu_3\text{-}O)_2]^{18+}$ or $[Mo_4(\mu_3\text{-}OR)_2]^{22+}$ unit for the class of clusters. A major structural consequence of cluster reduction in III and the neutral species $[Mo_4O_6(n\text{-}OC_3H_7)_6Cl_4]$ is a reduction of the cluster volume as a result of contraction in two sets of Mo–Mo bonds.

The structure of the catecholate derivative $[n\text{-}Bu_4N]_2[Mo_4O_{10}(OCH_3)_2(OC_6H_4O)_2]$ ($[n\text{-}Bu_4N]_2$[IVa]) is derived from that of I by substitution of a terminal and a bridging methoxo group on each of two Mo centers of I by the catecholate ligands. A key feature of the structure of IVa is the retention of the tetranuclear core with pseudooctahedral $[MoO_6]$ coordination geometries, as shown in Figure 8. Although a number of Mo–catecholato and related complexes have been previously structurally characterized,[46-51] IVa is a unique example of the tetranuclear core, emphasizing the dramatic influence of reaction conditions on the structural chemistry of oxomolybdate(VI) species.

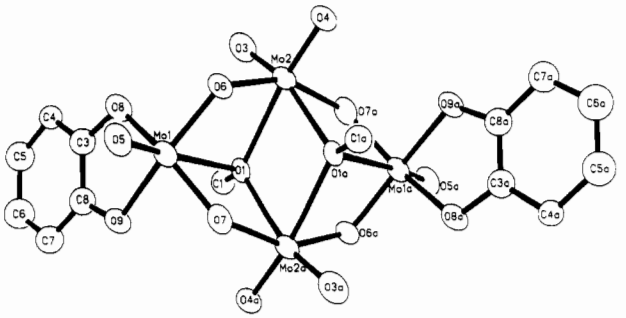

Figure 8. Perspective view of the structure of $[Mo_4O_{10}(OCH_3)_2(OC_6H_4O)_2]^{2-}$ (IVa), showing the atom-labeling scheme.

The structural parameters associated with IVa are similar to those of I, although some structural reorganization is obvious from

(46) Cass, M. E.; Pierpont, C. G. *Inorg. Chem.* **1986**, *25*, 123.
(47) Buchanan, R. M.; Pierpont, C. G. *Inorg. Chem.* **1979**, *18*, 1616.
(48) Pierpont, C. G.; Buchanan, R. M. *Inorg. Chem.* **1982**, *21*, 652.
(49) Pierpont, C. G.; Buchanan, R. M. *J. Am. Chem. Soc.* **1975**, *97*, 6450.
(50) Pierpont, C. G.; Downs, H. H. *J. Am. Chem. Soc.* **1975**, *97*, 423.
(51) Griffith, W. P.; Pumphrey, C. A.; Skapski, A. C. *Polyhedron* **1987**, *6*, 891.

Table X. Selected Bond Lengths (Å) and Angles (deg) for $[n\text{-Bu}_4\text{N}]_2[\text{Mo}_4\text{O}_{10}(\text{OCH}_3)_2(\text{OC}_6\text{H}_4\text{O})_2]$ ($[n\text{-Bu}_4\text{N}]_2$[IVa])

Mo1–O1	2.416 (7)	Mo3–O2	2.421 (7)
Mo1–O5	1.699 (8)	Mo3–O12	1.697 (8)
Mo1–O6	1.817 (7)	Mo3–O13	1.853 (8)
Mo1–O7	1.824 (9)	Mo3–O14a	1.837 (8)
Mo1–O8	1.981 (9)	Mo3–O15	1.981 (8)
Mo1–O9	1.982 (7)	Mo3–O16	2.005 (9)
Mo2–O1	2.270 (7)	Mo4–O2	2.235 (7)
Mo2–O1a	2.248 (8)	Mo4–O2a	2.254 (7)
Mo2–O3	1.682 (11)	Mo4–O10	1.696 (9)
Mo2–O4	1.677 (8)	Mo4–O11	1.686 (9)
Mo2–O6	1.983 (7)	Mo4–O13	1.966 (8)
Mo2–O7a	1.990 (8)	Mo4–O14	1.984 (8)
O1–Mo1–O5	170.7 (3)	O1–Mo3–O12	171.8 (4)
O6–Mo1–O9	153.8 (3)	O13–Mo3–O15	154.4 (3)
O7–Mo1–O8	155.4 (3)	O14a–Mo3–O16	153.7 (3)
O8–Mo1–O9	77.1 (3)	O15–Mo3–O16	77.4 (3)
O6–Mo2–O7	100.5 (4)	O2–Mo4–O10	158.8 (3)
O1–Mo2–O4	161.4 (4)	O2a–Mo4–O11	161.5 (4)
O1a–Mo2–O3	159.9 (4)	O2–Mo4–O14	154.3 (3)
O6–Mo2–O1a	152.7 (4)	O2–Mo4–O2a	69.2 (3)
O1–Mo2–O1a	68.4 (3)	O10–Mo4–O11	106.3 (5)
O3–Mo2–O4	104.8 (5)		

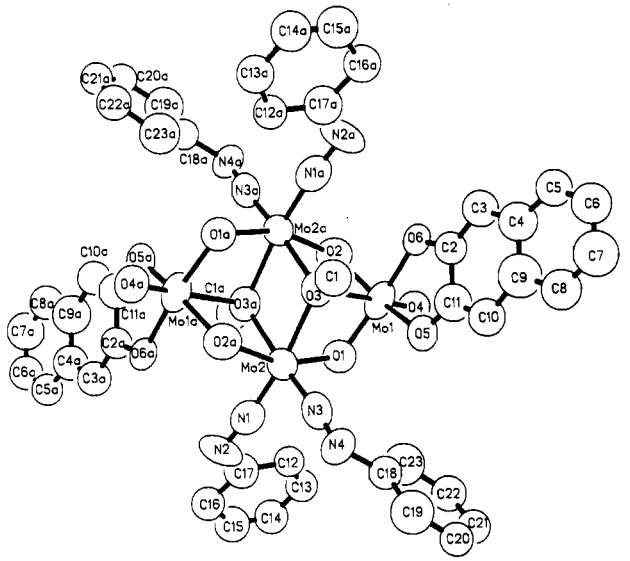

Figure 9. View of the structure of $[\text{Mo}_4\text{O}_6(\text{OCH}_3)_2(\text{C}_{10}\text{H}_6\text{O}_2)_2(\text{NNC}_6\text{H}_5)_4]^{2-}$ (Vc), showing the atom-labeling scheme.

the polyhedron models shown in Figure 4. However, the $[\text{Mo}_4(\mu\text{-OCH}_3)_2]$ core is maintained in IVa, illustrating that considerable variation in the peripheral ligands does not dramatically alter the core unit.

A novel structural feature associated with IVa is the absence of the two short–two intermediate–two long Mo–O distances for Mo1, generally observed for polyoxomolybdate structures. As listed in Table X, the Mo center coordinated to the catecholate ligand exhibits one short Mo–terminal oxo distance (1.699 (8) Å), one long Mo–methoxo oxygen distance (2.416 (7) Å), unexceptional Mo–aryloxo type distances to the bidentate ligand (1.982 (9) Å, average), and relatively short Mo–bridging oxo distances (1.821 (10) Å, average). In contrast, the 2 + 2 + 2 pattern is retained for Mo2. One consequence of this bonding pattern is the inequivalence of the Mo–O distances in the $[\text{Mo}_4\text{O}_4]$ heterocycle, common to structures of types IV and V.

The consequences of introducing strong π-bonding nitrogen donor ligands are illustrated by the structure of $[n\text{-Bu}_4\text{N}_2]$-$[\text{Mo}_4\text{O}_6(\text{OCH}_3)_2(\text{C}_{10}\text{H}_6\text{O}_2)_2(\text{NNC}_6\text{H}_5)_4]$ ($[n\text{-Bu}_4\text{N}]_2$[Vc]), depicted in Figure 9. The tetranuclear cluster is again situated on a center of symmetry, with the unique molybdenum centers exhibiting significantly different coordination geometries, $[\text{MoO}_6]$ for Mo1 and $[\text{MoO}_4\text{N}_2]$ for Mo2. The Mo1 center enjoys coordination to a single terminal oxo group, two doubly bridging oxo groups, the oxygen donors of the naphthalene-2,3-diolate ligand, and the triply bridging methoxo group. The Mo1–O3 distance is exceptionally long, 2.586 (8) Å, corresponding to a bond strength of approximately 0.15.[52] In fact, the coordination geometry about Mo1 approaches the square-pyramidal limit, with a weakly interacting sixth ligand, O3. In this description, the terminal oxo group, O4, occupies the apical position, while the base of the pyramid is defined by the bridging oxo groups O1 and O2 and the hydroxo donors O5 and O6. The Mo2 center displays more regular coordination of modified 2 + 2 + 2 variety with short Mo–N bonds to the two diazenido ligands, intermediate-length Mo–O bonds to the bridging oxo groups, and longer Mo–O bonds to the methoxo groups. The short bond lengths for the [Mo–N–N]

Table XI. Atomic Coordinates ($\times 10^4$) and Equivalent Isotropic Temperature Factors ($\text{Å}^2 \times 10^3$) for $[(\text{C}_4\text{H}_9)_4\text{N}]_2[\text{Mo}_4\text{O}_6(\mu_3\text{-OCH}_3)_2(\text{O}_2\text{C}_{10}\text{H}_6)_2(\text{NNC}_6\text{H}_5)_4]$ ($[n\text{-Bu}_4\text{N}]_2$[Vc])

	x	y	z	U_{eq}[a]
Mo1	8433 (1)	1605 (1)	782 (1)	91 (1)
Mo2	9096 (1)	2064 (1)	1714 (1)	84 (1)
O1	9014 (4)	1693 (4)	1130 (3)	86 (5)
O2	7821 (4)	1056 (4)	1064 (3)	91 (6)
O3	8343 (3)	2089 (4)	1460 (3)	94 (5)
O4	8484 (4)	1241 (4)	361 (3)	114 (6)
O5	8922 (5)	2435 (6)	629 (3)	85 (7)
O6	7856 (5)	1854 (6)	568 (3)	99 (7)
N1	9613 (5)	1868 (5)	1943 (4)	108 (7)
N2	9938 (7)	1700 (8)	2126 (6)	149 (12)
N3	9677 (6)	2777 (6)	1577 (4)	93 (9)
N4	10097 (7)	3264 (7)	1512 (4)	92 (9)
C1	8330 (7)	2620 (6)	1472 (5)	86 (9)
C2	8049 (11)	2409 (9)	432 (5)	106 (13)
C3	7768 (11)	2662 (14)	271 (6)	111 (20)
C4	7993 (19)	3218 (14)	155 (9)	112 (22)
C5	7736 (15)	3481 (13)	−6 (10)	124 (20)
C6	8010 (21)	4016 (22)	−127 (13)	188 (44)
C7	8532 (21)	4310 (16)	−97 (11)	153 (32)
C8	8809 (17)	4088 (17)	59 (10)	140 (26)
C9	8570 (19)	3527 (14)	209 (8)	106 (21)
C10	8920 (10)	3303 (10)	366 (6)	109 (14)
C11	8667 (11)	2728 (9)	481 (5)	102 (14)
C12	10077 (15)	1395 (13)	1405 (9)	173 (19)
C13	10413 (13)	1157 (13)	1284 (12)	136 (23)
C14	10733 (20)	988 (18)	1456 (14)	183 (32)
C15	10740 (12)	1008 (14)	1853 (15)	181 (30)
C16	10522 (10)	1261 (9)	2126 (9)	149 (16)
C17	10168 (8)	1430 (8)	1788 (12)	182 (17)
C18	10424 (8)	3354 (9)	1134 (5)	101 (12)
C19	10868 (9)	3935 (9)	1059 (6)	127 (13)
C20	11199 (9)	4044 (10)	693 (9)	126 (14)
C21	11094 (12)	3620 (15)	418 (7)	134 (21)
C22	10696 (10)	3091 (12)	489 (6)	114 (15)
C23	10331 (7)	2930 (9)	845 (6)	94 (11)
N5	6743 (6)	9235 (6)	833 (4)	103 (4)
C31	6958 (9)	9201 (8)	1257 (6)	120 (6)
C32	7018 (10)	8709 (9)	1380 (7)	124 (7)
C33	7106 (12)	8656 (13)	1788 (8)	133 (10)
C34	6909 (15)	8833 (15)	2093 (14)	124 (19)
C35	6151 (8)	8727 (9)	763 (6)	115 (7)
C36	5672 (9)	8636 (9)	1049 (7)	131 (8)
C37	5109 (12)	8139 (13)	1020 (10)	180 (14)
C38	4674 (13)	8026 (14)	1272 (9)	189 (16)
C39	6717 (8)	9776 (8)	804 (5)	111 (6)
C40	6530 (11)	9918 (10)	432 (7)	143 (8)
C41	6431 (10)	10453 (11)	427 (7)	145 (8)
C42	6040 (12)	10373 (14)	665 (9)	118 (12)
C43	7159 (8)	9224 (9)	521 (6)	133 (7)
C44	7785 (8)	9678 (10)	530 (7)	122 (7)
C45	8107 (18)	9631 (18)	271 (10)	140 (15)
C46	8742 (12)	10057 (13)	236 (10)	182 (16)

[a] Equivalent isotropic U defined as one-third of the trace of the orthogonalized $\mathbf{U}_{ij}$ tensor.

(52) Bart, C. J.; Ragaini, V. In *Proceedings of the Climax 3rd International Conference on the Chemistry and Uses of Molybdenum*; Davy, H. F., Mitchell, P. C. H., Eds.; Climax Molybdenum Co.: Ann Harbor, MI, 1979.

Table XII. Selected Bond Lengths (Å) and Angles (deg) for $[n\text{-Bu}_4\text{N}]_2[\text{Mo}_4\text{O}_6(\text{OCH}_3)_2(\text{C}_{10}\text{H}_6\text{O}_2)_2(\text{NNC}_6\text{H}_5)_4]$ ($[n\text{-Bu}_4\text{N}]_2$[Vc])

Mo1–O1	1.821 (9)	Mo2–O1	2.068 (8)
Mo1–O2	1.794 (9)	Mo2–O2	2.067 (8)
Mo1–O3	2.586 (8)	Mo2–O3	2.193 (8)
Mo1–O4	1.698 (9)	Mo2–O3a	2.182 (9)
Mo1–O5	1.982 (12)	Mo2–N1	1.849 (14)
Mo1–O6	2.069 (11)	Mo2–N3	1.800 (15)
Mo1···Mo2	3.356 (1)	N1–N2	1.293 (16)
Mo2···Mo2a	3.530 (1)	N3–N4	1.235 (15)
O1–Mo1–O6	151.6 (4)	N1–Mo2–O3	167.1 (4)
O2–Mo1–O5	148.6 (4)	N3–Mo2–O3a	173.1 (4)
O3–Mo1–O4	175.4 (4)	O1–Mo2–O2a	158.5 (3)
O1–Mo1–O2	99.6 (4)	N1–Mo2–N3	91.5 (5)
O5–Mo1–O6	75.1 (5)	O3–Mo2–O3a	72.4 (4)
O4–Mo1–O1	104.3 (4)	Mo2–N1–N2	174.9 (11)
O4–Mo1–O2	103.2 (4)	Mo2–N3–N4	174.9 (11)
O4–Mo1–O5	103.2 (4)		
O4–Mo1–O5	104.3 (4)		
O4–Mo1–O6	102.0 (4)		

moiety, together with the linearity of the grouping, confirm the description of the ligand as the phenyldiazenido group, formally the monopositive ligand $(C_6H_5NN)^+$.

Although structurally analogous to Vc, the *o*-aminophenolate derivative $[n\text{-Bu}_4\text{N}]_2[\text{Mo}_4\text{O}_6(\text{OCH}_3)_2(\text{OC}_6\text{H}_4\text{NH})_2(\text{NNC}_6\text{H}_5)_4]$ ($[n\text{-Bu}_4\text{N}]_2$[Vd]), shown in Figure 10, does display curious structural features. The most significant difference between the structures of Vc and Vd is revealed in the Mo1–O3 bond distances of 2.586 (8) Å for Vc and 2.698 (14) Å for Vd, a lengthening of ca. 0.10 Å. The Mo1 geometry, thus, most closely approximates the square-pyramidal, rather than the octahedral, limit.

As illustrated in Figure 11, a detailed comparison of the structural cores of I, Vc, Vd, and $[n\text{-Bu}_4\text{N}]_2[\text{Mo}_4\text{O}_8(\text{OCH}_3)_2(\text{NNC}_6\text{H}_5)_4]$ reveals that the $[\text{Mo}_4(\mu\text{-O})_4]$ ring common to these structures adopts a chair configuration with some degree of flexibility. The limiting cases are presented by $[\text{Mo}_4\text{O}_{10}(\text{OCH}_3)_6]^{2-}$ (I) and $[\text{Mo}_4\text{O}_8(\text{OCH}_3)_2(\text{NNC}_6\text{H}_5)_4]^{2-}$. The folding of the chair configuration of the $[\text{Mo}_4(\mu\text{-O})_2(\mu\text{-OCH}_3)_2]$ ring of I is pronounced as a consequence of the relatively strong Mo1–O6 interactions, 2.249 (2) Å, which draw the Mo1 centers into the central $[\text{Mo}_2(\mu_3\text{-OCH}_3)_2]$ rhombus. In contrast, the $[\text{Mo}_4(\mu\text{-O})_4]$ ring of $[\text{Mo}_4\text{O}_8(\text{OCH}_3)_2(\text{NNC}_6\text{H}_5)_4]^{2-}$ preesents a more shallow folding with the Mo1 and Mo3 centers displaced toward the $[\text{Mo}_4(\mu\text{-O})_4]$ best plane and exhibiting no bonding interaction with the methoxo groups of the $[\text{Mo}_2(\mu\text{-OCH}_3)_2]$ rhombus. The phenyl groups of the diazenido ligands are oriented so as to prevent close

Table XIII. Atom Coordinates ($\times 10^4$) and Temperature Factors ($\text{Å}^2 \times 10^3$) for $[\text{Bu}_4\text{N}]_2[\text{Mo}_4\text{O}_6(\text{OCH}_3)_2(\text{OC}_6\text{H}_4\text{NH})_2(\text{NNC}_6\text{H}_5)_4]$ ($[\text{Bu}_4\text{N}]_2$[Vd])

atom	*x*	*y*	*z*	U_{iso}[a]	atom	*x*	*y*	*z*	U_{iso}[a]
Mo1	10061 (1)	−40 (1)	8352 (1)	49 (1)*	C43	2295 (7)	5901 (9)	9219 (9)	111 (10)
Mo2	9739 (1)	814 (1)	9819 (1)	45 (1)*	C44	2272 (7)	5212 (9)	9346 (9)	112 (10)
Mo3	32 (1)	5402 (1)	5912 (1)	52 (1)*	C45	1834 (7)	4823 (9)	8764 (9)	104 (10)
Mo4	44 (1)	6265 (1)	4265 (1)	61 (1)*	C46	1418 (7)	5123 (9)	8056 (9)	83 (8)
N1	10083 (6)	1601 (7)	9895 (8)	36 (6)*	C51	−895 (8)	5473 (9)	7370 (9)	70 (7)
N2	10322 (7)	2168 (8)	10108 (10)	51 (7)*	C52	−1295 (8)	5753 (9)	7671 (9)	92 (8)
N3	9013 (7)	1200 (8)	9494 (10)	53 (7)*	C53	−1338 (8)	5499 (9)	8397 (9)	106 (10)
N4	8517 (7)	1407 (8)	9075 (11)	57 (7)*	C54	−982 (8)	4965 (9)	8821 (9)	115 (11)
N5	10510 (7)	779 (8)	8324 (10)	48 (8)*	C55	−583 (8)	4686 (9)	8521 (9)	116 (11)
N6	618 (6)	5837 (8)	6719 (10)	50 (6)*	C56	−539 (8)	4940 (9)	7795 (9)	96 (9)
N7	1036 (7)	6160 (8)	7197 (10)	54 (8)*	C61	1241 (8)	6687 (11)	5111 (14)	104 (9)
N8	−474 (9)	5568 (8)	6363 (10)	51 (9)*	C62	1255 (8)	6346 (11)	4415 (14)	88 (8)
N9	−815 (9)	5768 (9)	6688 (11)	70 (10)*	C63	1784 (8)	6277 (11)	4307 (14)	136 (12)
N10	715 (7)	6741 (8)	5195 (9)	49 (8)*	C64	2298 (8)	6550 (11)	4894 (14)	115 (11)
O1	10881 (7)	−387 (8)	8516 (10)	84 (8)*	C65	2284 (8)	6892 (11)	5589 (14)	119 (11)
O2	9679 (7)	−220 (7)	7324 (8)	68 (7)*	C66	1755 (8)	6960 (11)	5698 (14)	129 (12)
O3	10501 (5)	189 (5)	10018 (7)	42 (5)*	C80	688 (10)	1929 (11)	2621 (14)	68 (7)
O4	9594 (5)	530 (7)	8629 (7)	52 (5)*	C81	1112 (11)	2387 (13)	2449 (16)	82 (8)
O5	9976 (6)	777 (7)	11093 (8)	57 (7)*	C82	1511 (15)	1982 (17)	2171 (20)	125 (11)
O6	734 (7)	6123 (7)	3913 (8)	76 (8)*	C83	1952 (17)	2470 (18)	2011 (24)	147 (13)
O7	−366 (7)	6909 (6)	3686 (10)	80 (8)*	C84	−41 (10)	2883 (12)	2355 (14)	67 (7)
O8	546 (6)	5191 (5)	5139 (9)	51 (5)*	C85	−435 (11)	2664 (14)	1426 (17)	89 (8)
O9	−234 (6)	6183 (6)	5047 (8)	59 (6)*	C86	−563 (14)	3377 (16)	969 (20)	113 (10)
O10	−292 (5)	5527 (6)	3649 (8)	55 (6)*	C87	−1008 (17)	3218 (19)	62 (24)	153 (14)
C3	11085 (8)	460 (10)	10418 (13)	56 (9)*	C88	−188 (12)	1746 (14)	2971 (16)	94 (9)
C8	1156 (10)	5091 (11)	5504 (13)	66 (11)*	C89	−627 (14)	2012 (16)	3304 (19)	114 (10)
N11	267 (8)	2284 (8)	2927 (12)	73 (10)*	C90	−1231 (20)	1561 (23)	3034 (28)	196 (18)
N12	1414 (8)	8642 (10)	3674 (11)	73 (9)*	C91	−977 (23)	1023 (26)	3416 (34)	229 (22)
C11	10469 (7)	2591 (7)	9546 (9)	55 (6)	C92	606 (12)	2633 (14)	3789 (18)	92 (9)
C12	10634 (7)	3252 (7)	9790 (9)	75 (7)	C93	958 (13)	2130 (15)	4458 (18)	103 (9)
C13	10732 (7)	3696 (7)	9235 (9)	83 (8)	C94	1235 (18)	2452 (22)	5346 (26)	163 (15)
C14	10665 (7)	3480 (7)	8436 (9)	94 (9)	C95	1547 (25)	2922 (29)	5230 (34)	230 (23)
C15	10500 (7)	2820 (7)	8192 (9)	84 (8)	C101	789 (11)	8789 (12)	3520 (15)	76 (7)
C16	10402 (7)	2375 (7)	8748 (9)	64 (7)	C102	519 (12)	8345 (14)	4008 (17)	97 (9)
C21	8114 (7)	1588 (8)	9409 (11)	56 (6)	C103	−106 (14)	8533 (16)	3864 (21)	131 (12)
C22	7599 (7)	1889 (8)	8863 (11)	86 (8)	C104	−238 (18)	9231 (21)	4088 (25)	172 (15)
C23	7193 (7)	2144 (8)	9168 (11)	134 (12)	C105	1823 (11)	8701 (13)	4612 (16)	85 (8)
C24	7302 (7)	2096 (8)	10020 (11)	118 (11)	C106	1796 (14)	9380 (16)	4962 (20)	114 (10)
C25	7817 (7)	1795 (8)	10566 (11)	132 (12)	C107	2296 (16)	9416 (19)	5914 (24)	145 (13)
C26	8223 (7)	1541 (8)	10261 (11)	85 (8)	C108	2238 (22)	10095 (26)	6257 (31)	201 (19)
C31	11404 (9)	1259 (7)	8261 (12)	117 (11)	C109	1478 (12)	7921 (15)	3447 (17)	99 (9)
C32	11055 (9)	738 (7)	8348 (12)	76 (7)	C110	1135 (12)	7781 (15)	2496 (17)	99 (9)
C33	11259 (9)	79 (7)	8432 (12)	74 (7)	C111	1119 (15)	6996 (18)	2346 (21)	139 (12)
C34	11813 (9)	−59 (7)	8429 (12)	85 (8)	C112	1714 (17)	6848 (20)	2309 (24)	159 (14)
C35	12162 (9)	463 (7)	8342 (12)	102 (9)	C113	1571 (11)	9177 (13)	3122 (15)	77 (7)
C36	11957 (9)	1122 (7)	8259 (12)	125 (11)	C114	2231 (13)	9117 (15)	3204 (18)	107 (10)
C41	1440 (7)	5812 (9)	7929 (9)	68 (7)	C115	2352 (13)	9627 (16)	2626 (18)	104 (10)
C42	1879 (7)	6201 (9)	8510 (9)	76 (7)	C116	2279 (16)	10310 (18)	2845 (22)	142 (13)

[a] Values marked with an asterisk denote equivalent isotropic *U* values, defined as one-third of the trace of the orthogonalized U_{iso} tensor.

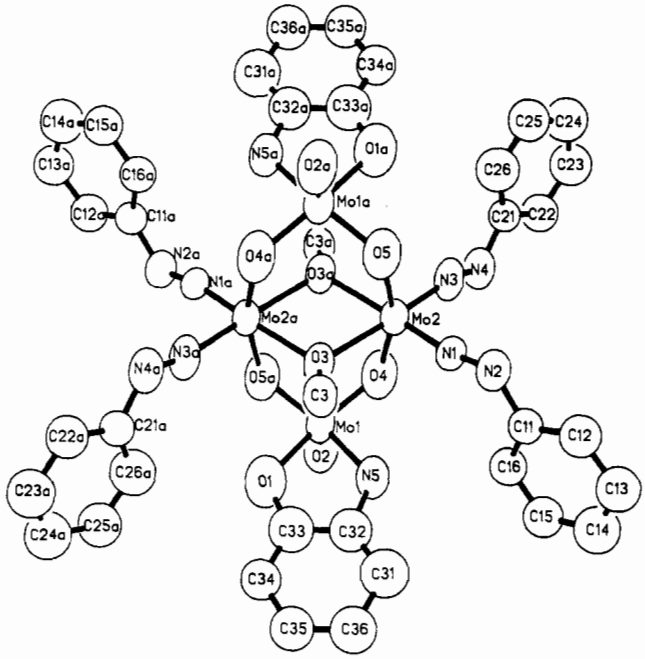

Figure 10. Perspective view of the structure of $[Mo_4O_6(OCH_3)_2(OC_6H_4NH)_2(NNC_6H_5)_4]^{2-}$ (Vd), showing the atom-labeling scheme.

Table XIV. Selected Bond Lengths (Å) and Angles (deg) for $[n\text{-}Bu_4N]_2[Mo_4O_6(OCH_3)_2(OC_6H_4NH)_2(NNC_6H_5)_4]$ ($[n\text{-}Bu_4N]_2$[Vd])

Mo1–O1	2.052 (17)	Mo2–O3	2.169 (12)
Mo1–O2	1.700 (12)	Mo2–O3a	2.136 (11)
Mo1–O3	2.698 (14)	Mo2–O4	2.031 (13)
Mo1–O4	1.809 (15)	Mo2–O5	2.051 (14)
Mo1–O5a	1.777 (14)	Mo2–N1	1.764 (15)
Mo1–N5	1.985 (16)	Mo2–N3	1.829 (17)
Mo4–O6	2.038 (19)	Mo3–O8	2.207 (17)
Mo4–O7	1.701 (13)	Mo3–O8a	2.180 (12)
Mo4–O8	2.639 (14)	Mo3–O9	2.081 (12)
Mo4–O9	1.743 (17)	Mo3–O10a	2.012 (12)
Mo4–O10	1.819 (12)	Mo3–N6	1.799 (13)
Mo4–N10	2.044 (14)	Mo3–N8	1.739 (23)
Mo1···Mo2	3.381 (1)	Mo3···Mo3a	3.488 (1)
Mo2···Mo2a	3.460 (1)	Mo3···Mo4	3.338 (1)
O1–Mo1–O4	150.4 (6)	O3–Mo2–N3	167.7 (6)
O5a–Mo1–N5	147.0 (5)	O3a–Mo2–N1	166.7 (5)
O2–Mo1–O1	101.1 (7)	O4–Mo2–O5	160.9 (5)
O2–Mo1–O4	104.9 (6)	O3–Mo2–O3a	73.0 (6)

approach of the Mo1 and Mo3 centers to the central rhombus. The structures of Vc and Vd display intermediate characteristics. Although the Mo1–O3 distance in Vc is significantly longer than the corresponding Mo1–O7 distance in I, the bond length is comparable to those observed in other structures with weakly

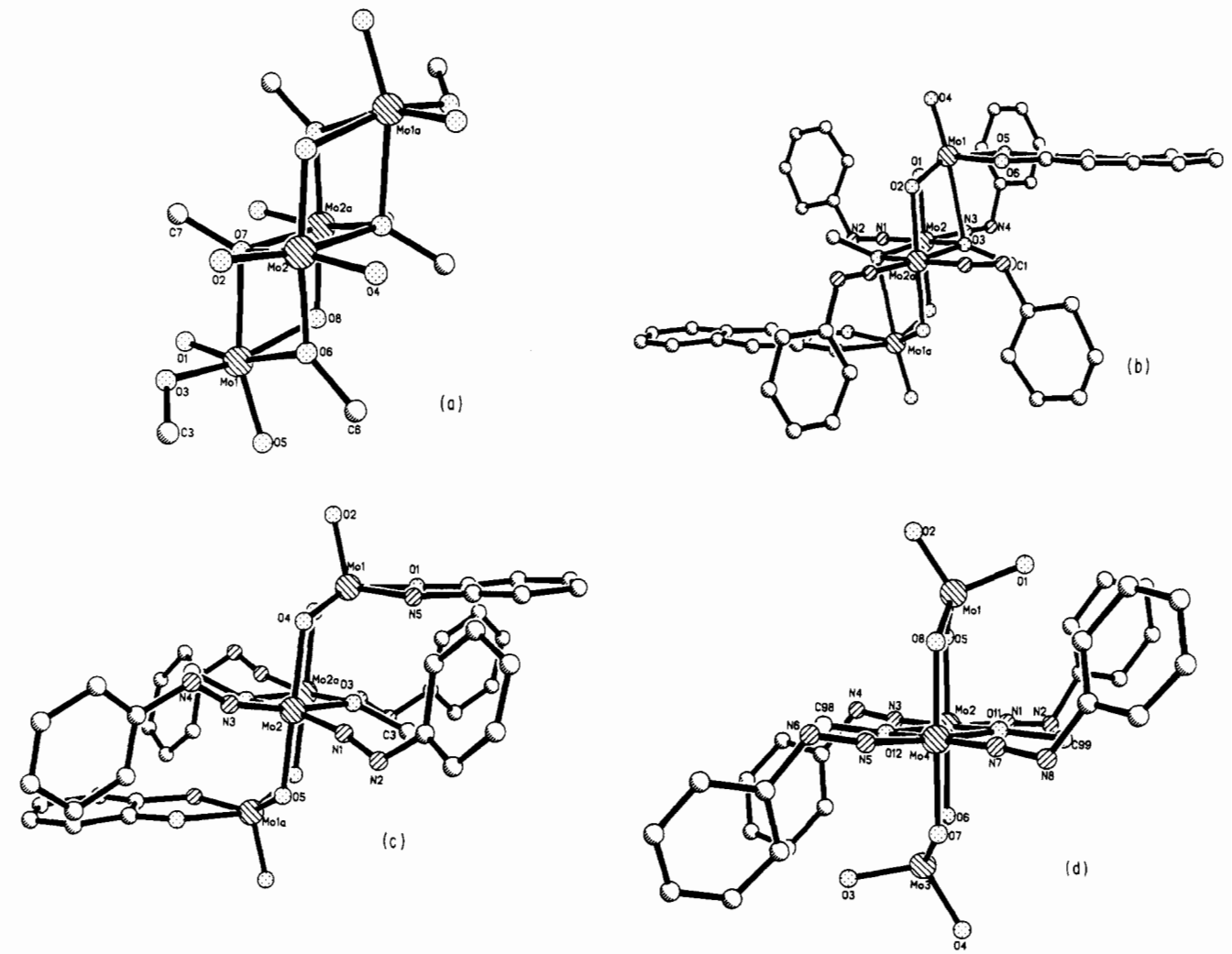

Figure 11. Comparison of the core structures of $[Mo_4O_{10}(OCH_3)_6]^{2-}$ (I), $[Mo_4O_6(OCH_3)_2(C_{10}H_6O_2)_2(NNC_6H_5)_4]^{2-}$ (Vc), $[Mo_4O_6(OCH_3)_2(OC_6H_4NH)_2(NNC_6H_5)_4]^{2-}$ (Vd), and $[Mo_4O_8(OCH_3)_2(NNC_6H_5)_4]^{2-}$, illustrating the structural flexibility associated with the coordination geometries of the units bridging the central $[Mo_2(OCH_3)_2O_4]^{2+}$ or $[Mo_2(OCH_3)_2(NNC_6H_5)_4]^{2+}$ cores. Whereas the structure of I is based on edge-shared $[MoO_6]$ octahedra and conforms to the empirical "rules of compactness",[56,57] the structure of $[Mo_4O_8(OCH_3)_2(NNC_6H_5)_4]^{2-}$ is constructed from corner-sharing $[MoO_4]$ tetrahedra and $[MoO_4N_2]$ units, resulting in a less compact aggregate. The structures of Vc and Vd are intermediate between these two limiting cases.

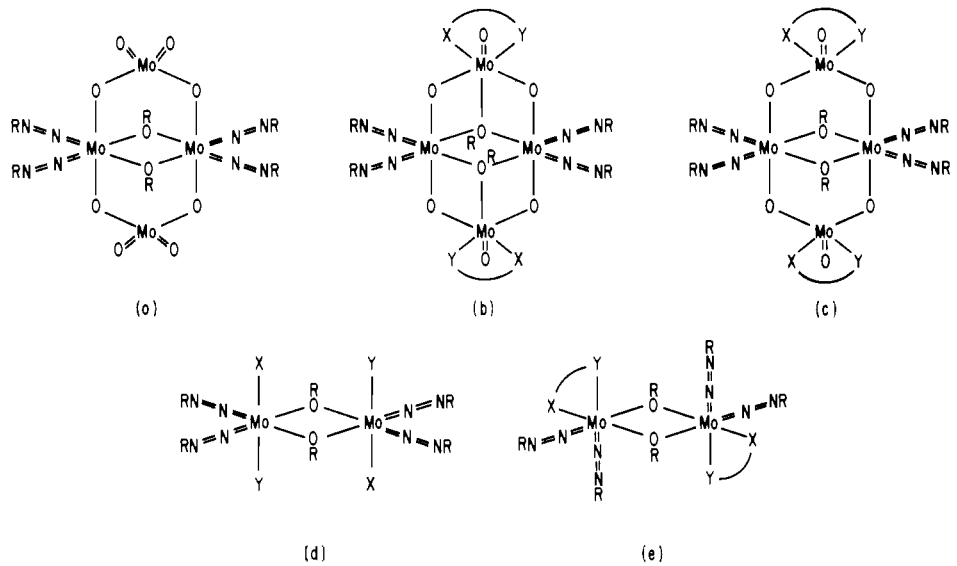

Figure 12. Schematic representation of structures possessing the $[Mo_2(OCH_3)_2(NNC_6H_5)_4]^{2+}$ core: (a) $[Mo_4O_8(OCH_3)_2(NNC_6H_5)_4]^{2+}$; (b) $[Mo_4O_6(OCH_3)_2(C_{10}H_8O_2)_2(NNC_6H_5)_4]^{2-}$ (Vc); (c) $[Mo_4O_6(OCH_3)_2(OC_6H_4NH)_2(NNC_6H_5)_4]^{2-}$ (Vd); (d) $[Mo_2(OCH_3)_2(NNC_6H_5)_4(X)(Y)]$, where X and Y are unidentate ligands; (e) $[Mo_2(OCH_3)_2(NNC_6H_5)_4(XY)_2]$, where XY is a bidentate ligand.

Table XV. Comparison of Selected Structural Parameters for Complexes Exhibiting the $[Mo_2(OCH_3)_2(NNC_6H_5)_4]^{2+}$ Core

	$[Mo_4O_8(OCH_3)_2(NNC_6H_5)_4]^{2-}$	Vc	Vd	$[Mo_2(OCH_3)_2(HOCH_3)_2(H_2NN(H)C_6H_5)_2(NNC_6H_5)_4]$	VId
Mo–N(diazenido), Å	1.821 (12)	1.825 (19)	1.797 (20)	1.824 (6)	1.819 (7)
Mo–(μ-OR), Å	2.140 (12)	2.188 (18)	2.152 (16)	2.117 (6)	2.172 (4), 2.065 (5)
Mo–OR–Mo, deg	107.4 (6)	106.2 (4)	107.0 (6)	107.1 (2)	107.6 (3)
N–Mo–N, deg	93.1 (6)	91.5 (5)	92.0 (7)	88.4 (3)	96.1 (2)
Mo–X, Å [X]	2.063 (12) [O]	2.068 (8) [O]	2.041 (17) [O]	2.264 (5) [N], 1.991 (5) [O]	2.269 (5) [N], 2.065 (5) [O]

Table XVI. Atom Coordinates (×10⁴) and Temperature Factors (Å² × 10³) for $[Mo_2(OCH_3)_2(OC_6H_4NH)_2(NNC_6H_5)_4]$ (VId)

atom	*x*	*y*	*z*	U_{iso}[a]
Mo1	848 (1)	566 (1)	3498 (1)	39 (1)
O1	1163 (4)	160 (4)	5314 (4)	42 (2)
O2	41 (5)	240 (4)	2197 (4)	45 (2)
N1	1341 (5)	−1521 (5)	4159 (5)	39 (3)
N2	2660 (6)	1022 (5)	2745 (5)	47 (3)
N3	3938 (7)	1291 (6)	2359 (5)	51 (3)
N4	169 (6)	2174 (6)	2984 (5)	43 (3)
N5	−446 (6)	3149 (5)	2880 (5)	46 (3)
C1	2498 (7)	−136 (8)	5804 (7)	65 (4)
C11	743 (6)	−1904 (6)	3344 (6)	38 (3)
C12	89 (7)	−948 (7)	2355 (6)	41 (3)
C13	−536 (7)	−1268 (7)	1561 (6)	50 (4)
C14	−493 (9)	−2511 (9)	1778 (8)	59 (5)
C15	157 (8)	−3465 (7)	2772 (7)	56 (4)
C16	762 (7)	−3135 (7)	3545 (7)	54 (4)
C31	4456 (7)	1435 (7)	1119 (6)	44 (3)
C32	3613 (7)	1306 (6)	339 (6)	48 (4)
C33	4204 (8)	1482 (7)	−845 (7)	59 (4)
C34	5591 (11)	1817 (9)	−1258 (9)	66 (5)
C35	6453 (8)	1906 (8)	−491 (8)	76 (5)
C36	5868 (8)	1725 (8)	716 (7)	64 (5)
C51	−1279 (7)	3831 (6)	1859 (6)	42 (3)
C52	−2237 (9)	4687 (7)	1973 (8)	63 (4)
C53	−3095 (10)	5357 (8)	1037 (9)	83 (5)
C54	−2927 (11)	5219 (10)	−47 (11)	81 (6)
C55	−1949 (9)	4371 (8)	−159 (8)	73 (5)
C56	−1126 (8)	3654 (7)	783 (7)	55 (4)
N6	3932 (8)	3370 (8)	4560 (7)	75 (4)
O3	5844 (7)	2435 (8)	5512 (7)	128 (5)
C2	5082 (10)	2723 (8)	4696 (10)	94 (6)
C3	3024 (14)	3669 (13)	3646 (13)	196 (13)
C4	3419 (13)	3766 (14)	5479 (12)	183 (11)

[a] Equivalent isotropic *U* defined as one-third of the trace of the orthogonalized U_{iso} tensor.

coordinating oxygen donors, 2.40–2.50 Å. Furthermore, the phenyl groups of the diazenido ligands have adopted relative orientations that minimize steric contacts with the 2,3-dihydroxynaphthalene ligands, allowing the Mo1 center to approach the O3 group. In contrast, the phenyl groups of Vd are oriented identically with those of $[Mo_4O_8(OCH_3)_2(NNC_6H_5)_4]^{2-}$, maximizing the steric interactions with the aminophenolate group and preventing a closer approach of the Mo1 center to the O3 methoxo group. Consequently, the Mo1–O3 distance is exceptionally long and is outside the range for a significant bonding interaction.

Table XVII. Selected Bond Lengths (Å) and Angles (deg) for $[Mo_2(OCH_3)_2(OC_6H_4NH_2)_2(NNC_6H_5)_4]$ (VId)

Mo1–O1	2.065 (5)	Mo1–N1	2.269 (5)
Mo1–O1a	2.172 (4)	Mo1–N2	1.815 (5)
Mo1–O2	2.036 (6)	Mo1–N4	1.823 (6)
N2–N3	1.242 (8)	N4–N5	1.227 (9)
Mo1···Mo1a	3.393 (1)		
O1–Mo1–O2	154.4 (2)	Mo1–N2–N3	173.1 (5)
N2–Mo1–O1a	170.6 (2)	Mo1–N4–N5	166.9 (4)
N1–Mo1–N4	171.1 (2)		
O1–Mo1–O1a	73.6 (2)		
N1–Mo1–O2	77.8 (2)		
N2–Mo1–N4	96.1 (2)		

The general structural parameters associated with Vc and Vd are similar and may be compared to other examples of structures with the $[Mo_2(OCH_3)_2(NNC_6H_5)_4]^{2+}$ core as shown in Table XV. The overall geometry of Vc may be viewed as two edge-sharing $[MoO_2(OMe)_2(NNC_6H_5)_2]$ octahedra bridged by edge-sharing tripodal $[MoO_3(OR)(C_{10}H_6O_2)]$ octahedra. In contrast, the structure of Vd consists of the same core of edge-sharing $[MoO_2(OCH_3)_2(NNC_6H_5)_2]$ octahedra, bridged by corner-sharing dipodal $[MoO_3(OC_6H_4NH)]$ square-pyramidal units. The structural diversity of the tetranuclear core receives significant emphasis in comparing these structures, Vc and Vd, with that of $[Mo_4O_8(OCH_3)_2(NNC_6H_5)_4]^{2-}$, which exhibits the identical core of edge-sharing $[MoO_2(OCH_3)_2(NNC_6H_5)_2]$ octahedra with corner-sharing dipodal $[MoO_4]$ tetrahedra completing the tetranuclear structure. The relationship of the tetranuclear units is represented schematically in Figure 12 and compared to binuclear structures with the $[Mo_2(OCH_3)_2(NNC_6H_5)_4]^{2+}$ core.

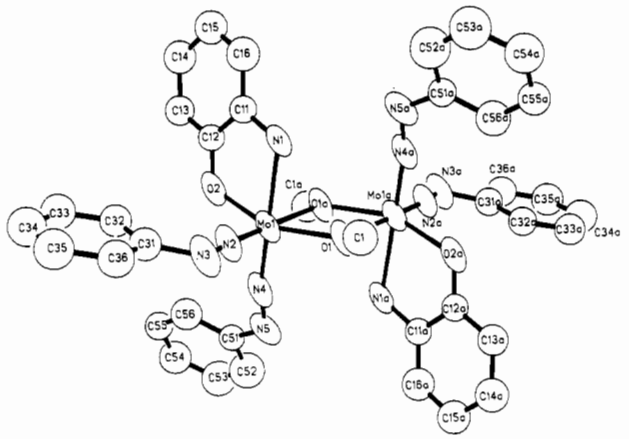

Figure 13. Perspective view of the structure of $[Mo_2(OCH_3)_2(NNC_6H_5)_4(OC_6H_4NH_2)_2]$, showing the atom-labeling scheme.

The complex $[Mo_2(OCH_3)_2(NNC_6H_5)_4(OC_6H_5NH_2)_2]$ (VId), shown in Figure 13, exhibits a structure representative of binuclear complexes of the class $[Mo_2(OR)_2(NNR)_4(LL)_2]$, where LL is a bidentate ligand. The structure of VId consists of discrete binuclear units with a center of symmetry at the centroid of the Mo1–Mo1a vector relating the Mo centers and imposing planarity on the Mo1–O1–Mo1a–O1a rhombus. The structural parameters associated with the $[Mo_2(OCH_3)_2(NNC_6H_4)_4]^{2+}$ core are similar to those observed for the series of tetranuclear and binuclear complexes possessing this core, as shown in Table XV.

The binuclear class of complexes displays two major structural variants, illustrated in Figure 12.[53] In those cases where the molybdenum coordination is completed by unidentate ligands, the phenyldiazenido ligands are mutually cis and the $[Mo_2(OR)_2(NNR)_4]^{2+}$ core is planar, while bidentate ligands impose the geometry associated with VId, in which two phenyldiazenido ligands assume an anti configuration relative to the planar $[Mo_2(OCH_3)_2(NNC_6H_5)_2$ unit. One consequence of the cis orientation of two diazenido groups relative to the bridging methoxo groups of the core is the dissymmetry of the methoxo bridges of the $[Mo_2(OCH_3)_2(NNC_6H_5)_4(LL)_2]$ class of binuclear structures. The pronounced trans influence of the strongly π-bonding diazenido ligand results in a significantly longer Mo–O(methoxo) distance of 2.172 (4) Å, relative to a value of 2.065 (5) Å for the Mo–O(methoxo) bond trans to the amino nitrogen, which exerts a negligible trans influence. In contrast, the structures of $[Mo_2(OCH_3)_2(NNC_6H_5)_4(X)_2(Y)_2]$, where X and Y are unidentate ligands, display nearly symmetrical methoxo bridges as a consequence of the cis in-plane arrangements of the diazenido ligands.

Conclusions. The tetranuclear polyoxomolybdate core represents a persistent chemical unit in methanolic solution, allowing a variety of ligand substitution reactions and even redox chemistry. $[n\text{-}Bu_4N]_2[Mo_4O_{10}(OCH_3)_6]$ ($[n\text{-}Bu_4N]_2[I]$) provides a synthetic precursor for a variety of tetranuclear complexes illustrated in Figure 1 and represents a structural prototype for the series of tetranuclear clusters.

Displacement of peripheral ligands associated with structure I allows synthesis of the related chloride and catecholate complexes $[n\text{-}Bu_4N]_2[Mo_4O_{10}(OCH_3)_4Cl_2]$ ($[n\text{-}Bu_4N]_2[II]$) and $[n\text{-}Bu_4N]_2[Mo_4O_{10}(OCH_3)_2(OC_6H_4O)_2]$ ($[n\text{-}Bu_4N]_2[IVa]$), respectively. Complexes of the type IV in turn provide precursors in the isolation of the series of complexes possessing the $[Mo_2(OCH_3)_2(NNC_6H_5)_4]^{2+}$ core, represented by $[n\text{-}Bu_4N]_2[Mo_4O_6(OCH_3)_2(NNC_6H_5)_4(LL)_2]$ ($[n\text{-}Bu_4N]_2[Va\text{–}d]$), where LL is a bidentate dianionic ligand.

The persistence and flexibility of the tetranuclear core is demonstrated by the variety of structural modifications encountered in the structures of I, II, IVa, Vc, and Vd. Furthermore, the isolation of the reduced tetranuclear species $[Et_3NH]_2[Mo_4O_8(OCH_3)_4Cl_4]$ ($[Et_3NH]_2[III]$) by chemical reduction of I demonstrates that the basic core may also accommodate reduced metal sites and concomitant cluster reorganization and contraction.

A common structural feature of the tetranuclear species is weak axial interactions between the central binuclear core $[Mo_2(OCH_3)_2(L_1)_2(L_2)_2]$ of edge-fused octahedra and the peripheral molybdate units. Consistent with this observation is the isolation of a variety of binuclear species under appropriate conditions. Binuclear complexes of the classes $[Mo_2(OCH_3)_2(NNC_6H_5)_4(X)_2(Y)_2]$ and $[Mo_2(OCH_3)_2(NNC_6H_5)_4(LL)_2]$ retain the chemically robust $[Mo_2(OCH_3)_2(NNC_6lH_5)_4]^{2+}$ core with peripheral ligand groups completing the pseudooctahedral Mo geometry.

Acknowledgment. We are grateful to the National Science Foundation for financial support (Grant No. CHE8514634 to J.Z.).

Registry No. $[Ph_3MeP]_2[I]$, 111496-03-8; $[n\text{-}Bu_4N]_2[II]$, 111496-05-0; $[Et_3NH]_2[III]$, 118681-93-9; $[n\text{-}Bu_4N]_2[IVa]$, 111496-07-2; $[n\text{-}Bu_4N]_2[IVb]$, 118681-95-1; $[n\text{-}Bu_4N]_2[IVc]$, 118681-97-3; $[n\text{-}Bu_4N]_2[IVd]$, 118681-99-5; $[n\text{-}Bu_4N]_2[Va]$, 118682-01-2; $[n\text{-}Bu_4N]_2[Vb]$, 118682-03-4; $[n\text{-}Bu_4N]_2[Vc]$, 118682-05-6; $[n\text{-}Bu_4N]_2[Vd]$, 114691-21-3; $[n\text{-}Bu_4N]_2[VIa]$, 118682-07-8; $[n\text{-}Bu_4N]_2[VIb]$, 118682-09-0; $[n\text{-}Bu_4N]_2[VIc]$, 118682-11-4; VId, 118682-13-6; $[Ph_3MeP][Mo_8O_{26}]$, 111496-08-3; α-$[n\text{-}Bu_4N]_4[Mo_8O_{26}]$, 59054-50-1; $[n\text{-}Bu_4N]_2[Mo_4O_8(OCH_3)_2(NNC_6H_5)_4]$, 104153-98-2; $[n\text{-}Bu_4N][MoO_2(C_6H_5(H)NNC(O)NNC_6H_5)(C_6H_5NNC(O)NNC_6H_5)]$, 114680-98-7.

Supplementary Material Available: Tables S1, S6, S11, S16, S21, S26, and S31, listing bond lengths, Tables S2, S7, S12, S17, S22, S27, and S32, listing bond angles, and Tables S3, S8, S13, S18, S23, S28, and S33, listing anisotropic temperature factors, for I–III, IVa, Vc, and VId, and Tables S4, S9, S14, S19, S24, and S34, listing calculated hydrogen atom positions, for I–III, IVa, Vc, and VId, and Table S36, listing experimental conditions for the data collection for all structures reported herein (44 pages); Tables S5, S10, S15, S20, S25, S30, and S35, listing calculated and observed structure factors for I–III, IVa, Vc, Vd, and VId (206 pages). Ordering information is given on any current masthead page.

(53) Carrillo, D.; Gouzerh, P.; Jeannin, T. *Nouv. J. Chim.* **1985**, *9*, 749.
(54) Hsieh, T.-C.; Zubieta, J. *Inorg. Chim. Acta* **1987**, *127*, L31.
(55) Chilou, V.; Gouzerh, P.; Jeannin, Y.; Olivares, G.; Robert, F.; Hsieh, T.-C.; Liu, S.; Zubieta, J. *Polyhedron*, in press.
(56) Kepert, D. L. *Inorg. Chem.* **1969**, *8*, 1556.
(57) Gaiffon, A.; Spinner, B. *Rev. Chim. Miner.* **1975**, *12*, 316.